Physical modelling of a sheet pile - vegetation system

Reuben Joseph

in partial fulfilment of the requirements for the degree of
Master of Science
in Civil Engineering
Delft University of Technology
April 2021

Student number: 4743997

Thesis Committee:
Prof. Dr. Ir. Cristina Jommi
Prof. Dr. Ir. J.W.G. van de Kuilen
Drs. W.F.Gard
Ir. Abhijith Kamath

CONTENTS

ACKNOWLEDGEMENT

This thesis marks the culmination of my student life at TU Delft. The thesis fitted my research interests perfectly while challenging my technical knowledge and problem-solving capabilities at every stage. I am forever indebted to Prof. Dr. Ir. Cristina Jommi for her help throughout my thesis. Her invaluable suggestions, patience, and support in my thesis and my coursework have helped me become a better student and a professional. I am honored to have worked under her guidance.

I am extremely grateful to Ir. Abhijith Kamath for all the help and guidance he provided throughout my thesis work. I am also grateful for all the extra work he put in, assisting me in the lab with the test setup. In addition to being a very accessible and helpful supervisor, he was also a good friend who helped me through the difficult times in my study. Thank you also for all the free coffee.

I would also like to thank Prof. Dr. Ir. Jan Willem van de Kuilen and Drs. Wolfgang Gard for giving me the opportunity to work under their guidance, and for the invaluable suggestions they provided during the thesis work.

I would like to thank the technicians at the Stevinweg 2 lab, in specific: Ing. Kees van Beek, Louis den Breejen and Micheal van der Meer, for helping me develop the test setup and for assisting me while performing the tests. I would also like to thank Ing. Wim Verwaal for his help with the lab tests in the Geo-Engineering laboratory.

My friends Kaushik, Akshayaa, Meera, Chris, Narasimhan, and Lee have always been there for me when I needed moral support. I am thankful to them.

Lastly and most importantly, I would like to thank my parents, Joseph and Elizabeth, and my brother, Rohith, for their love, support, and encouragement through the years. This would have been only a dream without their support. I am forever in their debt.

1

INTRODUCTION

1.1. BACKGROUND

CANTILEVER sheet pile walls are used for retaining granular soil in river protection walls, excavation and as temporary supports in foundation construction. Sheet pile walls resist the overturning moment due to the pressure from the soil retained (active pressure) by developing a restraining moment due to the passive pressure at the base along the embedment depth of the sheet pile wall (G.L.S. Babu and B.M. Basha, 2008). The materials commonly used to make sheet piles are steel and timber. About 60 percent of the 4000 km engineered sheet-pile retaining systems used to protect stream banks in the Netherlands are made of timber (Van de Kuilen and Van der Linden, 1999). While timber sheet-piles are effective in stabilizing the stream banks, timber is an organic material which can decay with time. Replacing these sheet-piles is a process that involves a lot of effort. Hence, more efficient alternatives are being investigated to address this problem.

Soil bio-engineering or eco-engineering is a practice that involves the use of vegetation to stabilize slopes. This practice provides an immediate stabilization of the soil, as well as long term stabilization due to the reinforcement effects of the roots on the soil. Vegetation can improve the stability of a slope by mechanical and hydrological mechanisms. There is an initial stress transfer between the soil and the structure but this is replaced in time with the evolving role of the vegetation. Once the vegetation becomes fully established, it takes on more of the functional role of the inert members in the system (Gray and Sotir, 1996). The mechanical reinforcement is provided by the roots, which transfer the shear stresses in the soil to the tensile stresses in the roots (Khalilnejad et al, 2012). The hydrological mechanism of reinforcement involves the reduction of pore-pressures in the soil through the uptake of water into the roots. The resulting negative pore-pressure helps increase the shear strength of the soil (Liu et al, 2016).

The root architecture also plays an important role in improving the strength of the soil-vegetation bio-engineering system. Liu et al (2016) noted that the exponential root architecture provided the the highest negative pore pressure in the soil at shallow depths,

thus increasing the strength of the soil at shallow depths. Soil bio-engineering has inherent advantages over the classical civil engineering solutions in terms of easy of construction, low landscape impact and the ability to offer an environment friendly alternative.

1.2. NEED FOR STUDY

Numerous studies have been carried out to understand the effects of vegetation reinforcement of slopes through centrifuge modelling (Schwarz et al, 2010; Pollen and Simon, 2005; Liang et al, 2015). There have also been studies to understand the behaviour of retaining structures through physical modelling (Viswanandham et al, 2016; Tricarico et al, 2016).

Previous studies were conducted using centrifuges at higher gravity, owing to the difficulty in making a 1g physical model and the time required for the vegetation to grow.Centrifuge tests subject models to centripetal accelerations which are many times greater than the earth's gravitational acceleration (Viswanandham et al, 2007). This helps create stress states in the model which are comparable to the stress states in the prototype. There have been studies which involved the use of live plants in a centrifuge to model slope failure and to understand the extent of root reinforcements in slopes (Sonnenberg et al, 2010; Askarinejad and Springman, 2015). Centrifuge tests have been conducted using 3D printed roots to understand the seismic performance of vegetated slopes, in an effort to boost the repeat-ability of tests (Liang, 2015).

While centrifuge tests are generally fast and accurate, there have been problems with over-estimation of the tensile strength of the roots in centrifuge tests, through scaling laws (Liang et al, 2017; Mickovski, 2009). This over-estimation of root tensile strength could lead to the over-estimation of root reinforcement and its contribution to slope stability.

1-g physical modelling helps avoid scaling errors by being able to represent the same physical properties in the model as in the prototype, thus giving a more reliable insight into the behaviour of the bio-engineering system. Hence, this study aims to contribute to the existing knowledge on the behaviour of bio-engineering systems, through 1g modelling.

1.3. RESEARCH OBJECTIVES

The objectives of this study are:

1. Understanding the effect of inclusion of vegetation in a sheetpile retaining system.
2. Understanding the influence of root area on enhancing the stability of stream banks with sheet-piles.

1.4. RESEARCH QUESTIONS

Based on the research objectives, the following research questions were formulated:

1. What is the effect of inclusion of vegetation in a sheetpile retaining system ?
2. What is the influence of spatial distribution and root area on the increase in stability of stream banks with sheet piles ?
3. Does the equivalent cohesion approach capture the effect of vegetation in a numerical model?

1.5. STRUCTURE OF THE REPORT

This report is organized as five chapters, progressing from focus on the prerequisite knowledge to the application of the acquired knowledge and analysing the results. The first chapter gives a basic introduction into the study, briefly outlining the existing knowledge on sheet-piles and bio-engineered retaining systems. This chapter also underlines the need for this study and lists the questions that were focused on in this study. The second chapter reviews the background literature, discussing the basic concepts involved in the design of a sheetpile system and concepts of bio-engineering. The third chapter discusses the methodology of the testing process, the components of the test setup, the method of fabrication of the root analogues, the testing procedure and the results of the tests. The fourth chapter discusses the modelling of the experiment in PLAXIS and assesses the ability to reproduce the results obtained in the experiments. The fifth and final chapter summarises the study, discusses the research questions and recommendations for future work.

2

BACKGROUND LITERATURE

2.1. INTRODUCTION

Sheet-piles are retaining structures which are used to retain materials like soil or water. Sheet-piles are used as waterfront structures in quays, piers or as river bank protection and also for retaining excavations. Sheet-piles are usually made of timber, steel or precast reinforced concrete. Timber sheet piles are widely used as temporary supports and for resisting light lateral loads. Timber sheet piles are also used for free-standing walls where the retaining height is less than 3m. Timber sheet-piles are joined to each other using a tongue and groove joint.

2.2. BASIC CONCEPTS

2.2.1. EARTH PRESSURES

Earth pressures are a reflection of stress states in the soil mass. Earth pressure is defined as the force per unit area exerted by the soil on the sheet-pile. The concept of earth pressure is represented by the earth pressure coefficient K. The earth pressure coefficient is the ratio of horizontal to vertical stresses at any depth in the soil mass.

$$K = \sigma_h / \sigma_v \tag{2.1}$$

The earth pressure for any given soil structure varies from an initial stress state called the at-rest pressure K_0, to the minimum limit state K_a or to the maximum limit state K_p.

At-rest pressure: This refers to a stress state where there is no lateral movement or strain in the soil mass. The earth pressures are similar to the pressures that existed in the ground prior to installation of the sheet pile. Hence the soil is in a state of static equilibrium.

$$K = K_0 = \sigma_h / \sigma_v \tag{2.2}$$

Active earth pressure: When the retaining wall moves away from the back-fill, a triangular soil mass adjacent to the sheet-pile wall slides downward toward the retaining wall.

The horizontal pressure exerted at this stage is called active earth pressure. Hence the equation becomes,

$$K = K_a = \sigma_a / \sigma_v \tag{2.3}$$

where σ_a is the active pressure.

Passive earth pressure: When the retaining wall moves towards the back-fill, a triangular mass of soil adjacent to the sheet-pile slides upward, away from the sheet-pile wall. The horizontal pressure exerted at this stage is called passive earth pressure.The horizontal earth pressure at this time will be $\sigma_h = \sigma_v$. This is the passive pressure.

$$K = K_p = \sigma_p / \sigma_v \tag{2.4}$$

2.3. CANTILEVER SHEET PILE WALLS

When sheet piles are fixed at the base and free at the top, they are called cantilever sheet piles. Cantilever sheet piles are used to retain moderate heights of 3m-5m. Cantilever sheet pile walls are used in flood walls, cut and fill projects and for protecting temporary and permanent excavations for highways and in landslide prone areas (Stanislav, 2006). Cantilever sheet piles depend on the embedment depth for stability. The lateral deflection of the sheet piles are huge because of the cantilever action.

2.3.1. MECHANICS OF A CANTILEVER SHEET PILE (DRY BACKFILL)

The sheet piles which are embedded in the soil are subjected to various forces exerted by the soil. The forces exerted on the sheet pile include:

1. The active earth pressure behind the sheet pile wall, which pushes the wall away from the back-fill.

2. The passive force developed in front of the wall, which resists the movements of the wall. The development of the passive force is due to the embedment of the sheet pile into the soil.

The active pressure acting on the back of the sheet-pile tries to push the wall away from the back-fill. An adequate embedment depth provides the resistance to the active pressure exerted by the wall. If the depth of embedment is adequate, then the cantilever sheet-pile rotates about a point O' which is called the point of transition (Murthy, 2011). The active and passive pressures acting along the different points on the sheet-pile are:

1. The active earth pressure Pa_1 acting at the back of the sheet-pile from the surface of the back-fill, down to the point of rotation O'.

2. The passive earth pressure Pp_1 acting in front of the wall, from the point of rotation O' to the dredge line.

3. The active earth pressure Pa_2 acting in front of the wall, from the point of rotation to the bottom of the wall.

4. The passive earth pressure Pp_2 acting at the back of the sheet-pile from the point of rotation O' to the bottom of the wall.

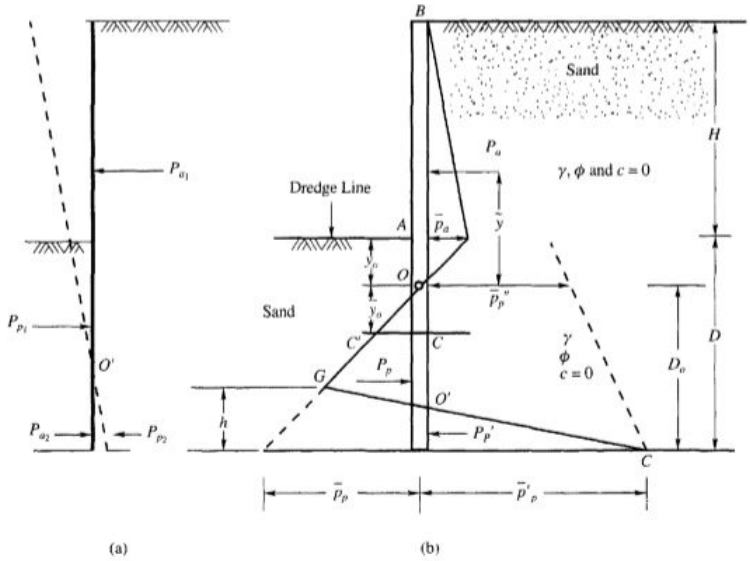

Figure 2.1: Pressure distribution on a cantilever sheet-pile wall.(Murthy, 2002)

The pressures acting on the wall are visualized in figure 2.1(a).The active and passive pressures algebraically combined, give a pressure distribution as depicted in figure 2.1(b).The notations used in the figure are:
D = minimum depth of embedment giving a factor of safety of 1
H = retaining height of the embankment
K_a = active earth pressure coefficient
K_p = passive earth pressure coefficient
P_a = effective active earth pressure acting at the dredge line = γ HK_a
P_p = effective passive earth pressure at the base of the sheet-pile wall and acting towards the back-fill =γ D0K_a
P_p' = effective passive earth pressure at the base of the sheet-pile acting against the back-fill side of the wall = P_p''+γ KD_0
P_p'' = effective passive earth pressure at level O = γ y_0K+γ HK

The stability of the cantilever sheet pile wall depends on the passive resistance that is produced by the soil in front of the wall, below the dredge level. The passive resistance depends on the depth of embedment provided to the sheet-pile and the density of the soil in front of the sheet-pile. The embedment depth of sheet piles for soils of different density is shown in table 2.1.

2.3.2. MECHANICS OF A CANTILEVER SHEET PILE WITH A WATER TABLE IN THE BACK-FILL

Sheet-pile structures installed near waterfront structures often have a water table within the back-fill. In such situations, the water table also contributes to the lateral pressures

Relative density	Embedment depth,D
Very loose	2.0H
Loose	1.5H
Firm	1.0H
Dense	0.75H

Table 2.1: Penetration depth of sheet-pile.(Source:Teng, 1969)

acting on the sheet-pile. For this condition, the submerged unit weight of the soil is considered for the lateral earth pressures. The earth pressure diagram for this condition in a cohesion less soil is showed in figure 2.2.

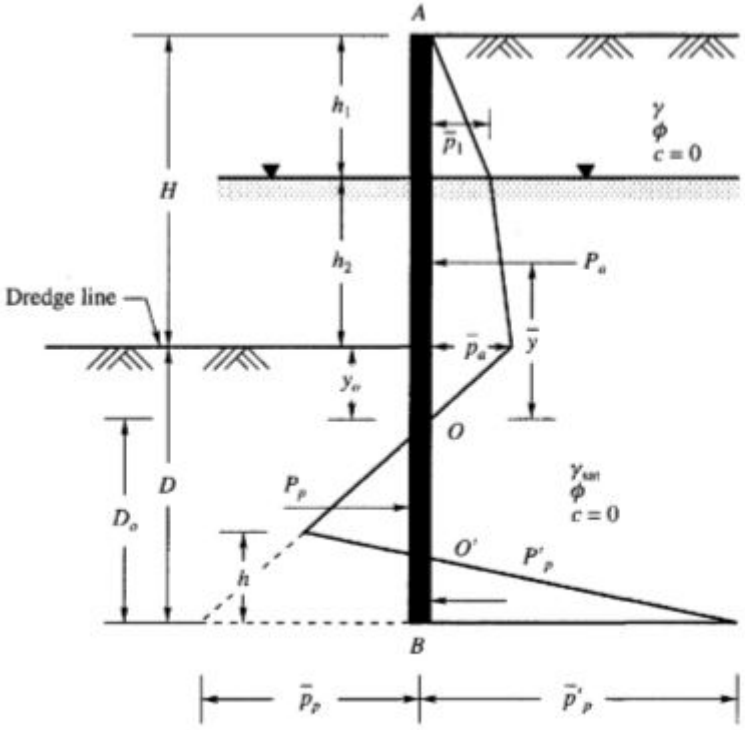

Figure 2.2: Pressure distribution on a cantilever sheet-pile wall with a water table in the back-fill.(After Murthy 2002)

EFFECT OF WATER TABLE ON STABILITY

Clayton et al (2014) summarized the effect of the water table on the stability of the embankment. The height of the water table in the back-fill is critical for the embedment depth provided. The are two mechanisms involved in this situation.

1. When the water table in the back-fill is at the same height as the water in the canal,

the effective stress levels in the soil decreases, as compared to the situation where the soil is above the ground water table. While there is a decrease in effective stresses, since K_a<1 and K_p>1, the active pressure in the back-fill increases while the passive resistance decreases. Hence, a longer embedment depth is required to counter the imbalance in forces, as compared to the situation where the water table is at a great depth.

2. When there is a difference in the water level in the active and the passive side, the net pressure results in a destabilizing force. Such effects are observed in areas where tidal effects are observed, like docks. In this case, a longer embedment depth would be required, as compared to the situation where the imbalance in forces does not exist.

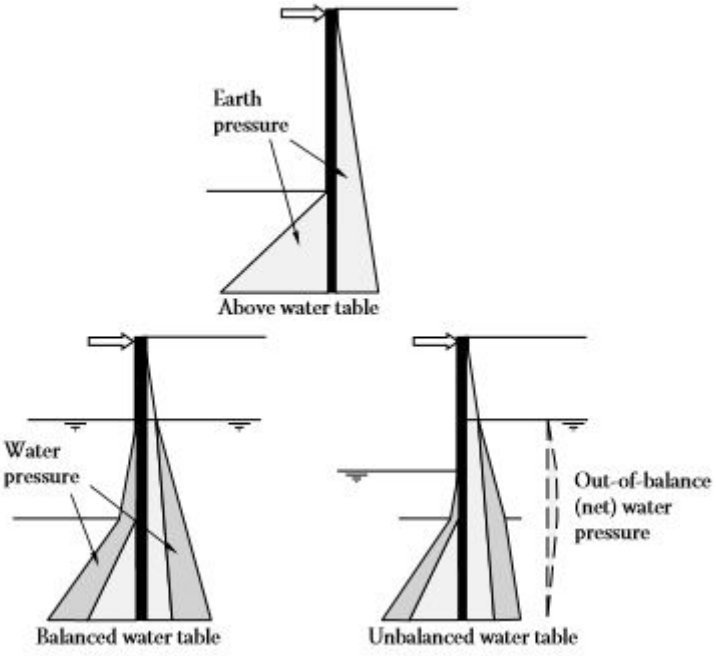

Figure 2.3: Effect of water level on the stability of the sheet pile

2.4. EFFECT OF VEGETATION ON SLOPE STABILITY

The banks of canals in The Netherlands and France have been reinforced with Willow roots since the Middle Ages (Van de Kuilen and Van der Linden, 1999). The contribution of plant roots to slope stability has been studied extensively in the past years by researchers, to understand the extent of the influence of roots in stabilizing slopes(khalilnejad et al, 2012; Mickovski et al, 2014; A.Cislaghi et al, 2017). This is potentially a cost-effective and environment friendly approach of stabilizing slopes (Gray and Sotir, 1996).

2.4.1. SOIL BIO-ENGINEERING

Morgan and Rickson (2003) defined bio-engineering as the use of any form of vegetation, whether singular or a collection of plants as an engineering material. Vegetation improves slope stability by improving the stability of the soil through hydrological and mechanical mechanisms.

HYDROLOGICAL REINFORCEMENT

The hydrological mechanism of soil reinforcement involves the modification of soil moisture content to increase the strength of the soil. This mechanism of reinforcement involves:

1. Reinforcement through evapotranspiration(ET).

2. Reinforcement through the root induced changes in hydraulic properties.

REINFORCEMENT THROUGH EVAPOTRANSPIRATION

Evapotranspiration is the loss of water from a given area, by evaporation from the soil surface and by transpiration from plants. Laboratory studies have shown that the drying effects brought about by evapotranspiration could induce a significant amount of matric suction, thus preserving suction in the soil (Pollen-Bankhead and Simon, 2010). Pollen-Bankhead and Simon (2010) showed that the effect of ET induced suction increased the FoS by 52 percent as compared to only a 25 percent increase in FoS through mechanical reinforcement. Ng et al (2016) measured the distribution of matric suction between bare and rooted slopes (Fig 2.4). It was observed that the amount of suction preserved below the root zone of the vegetated soil is always higher than that in the bare soil by 85 percent - 123 percent.

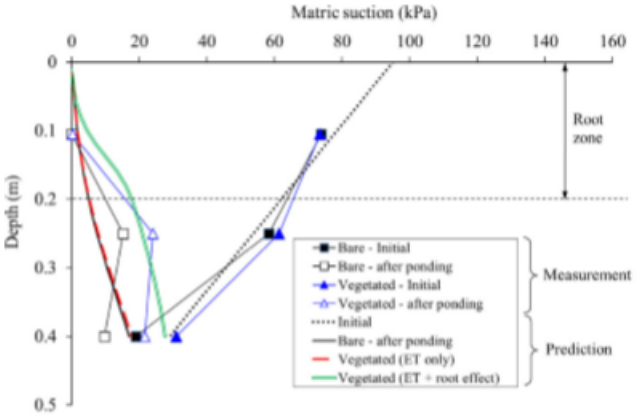

Figure 2.4: Comparison of measured and predicted suction before and after 2-h ponding for field tests conducted by Ng et al., (2016)

REINFORCEMENT THROUGH ROOT INDUCED CHANGES IN HYDRAULIC PROPERTIES

In addition to evapotranspiration, roots bring about the change in the soil water retention curve. Scholl et al (2014); Taleisnik et al (1999) and Traore et al (2000) conducted studies which showed that roots could change the structure of soil through:

1. Volumetric occupancy of roots in soil pore space.

2. Water retention in roots.

3. The release of root exudates.

Changes in soil structure would induce some changes in pore-size distribution and consequently the SWRC. J.J Ni et al (2017) investigated the influence of root induced modification of soil properties, on the stability of vegetated slopes. It was observed that, when only evapotranspiration is considered, the predicted suction profile in the vegetated soil is was found to be similar to the suction profile of the bare slope. But when the root induced changes in soil properties like SWRC and permeability are both considered, the predicted suction profiles for vegetated and bare slopes are similar to the measured suction profiles.

MECHANICAL REINFORCEMENT

The influence of mechanical reinforcement on the stability of slopes has been researched for over 40 years (Waldron, 1977; Gray and Sotir, 1996; Greenway, 1978; Coppin and Richards, 1990; Wu, 1995; Sonnenberg et al, 2010,2012; Liang, 2015) . Plant roots increase the shearing resistance of soil, by mechanical reinforcement of the soil. Waldron (1977) compared root reinforced soil to a composite material in which the material of high tensile strength (the root fibers) are embedded in a material with low tensile strength (the soil). Hence there is a transfer of mechanical energy from the roots to the soil. This additional reinforcement is thought to provide an additional 'apparent cohesion' to the soil.
Sonnenberg et al (2012) developed a centrifuge model to study the effect of vegetation on soil slopes. The study compared the performance of a bare slope and rooted slopes of varying root structures (tap root and branched root), subjected to higher stresses at 5g. It was observed that the presence of the tap root structures forced the failure plane deeper and changed the failure mechanism from a progressive block failure to an intact sliding block. The branched root pattern was more successful in stabilizing the slope by pushing the failure plant deeper.
The effect of reinforcement varies with plant species and root architecture. For shallow slopes, the function of roots is to increase the basal shear strength and this reinforcement decreases with increase in depth. The mechanical reinforcements of the roots is effective upto a depth of 0.5 m (JJ Ni et al, 2018).

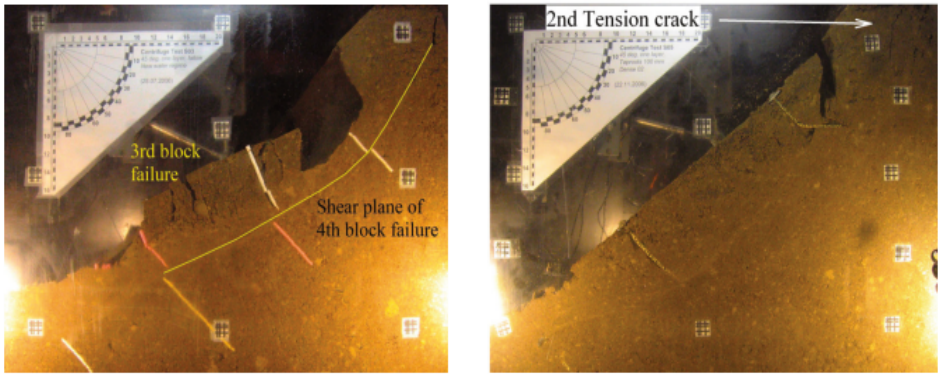

(a) Progressive block failure - bare soil.

(b) Intact sliding block - rooted soil

Figure 2.5: Comparison of failure planes observed in a bare slope and a rooted slope (Sonnenberg et al, 2011).

Schwarz et al (2010) summarized root diameter, root length, spatial arrangement and associated soil mechanical interactions as the root properties which affect the mechanical reinforcements of steep slopes. The increase in strength of root-reinforced soil had been solely attributed to these characteristics, while disregarding the effect of the properties of the surrounding soil. However, Duckett (2013), through parametric studies, observed a positive relationship between confining stress and root cohesion, as reported by Liang (2015).

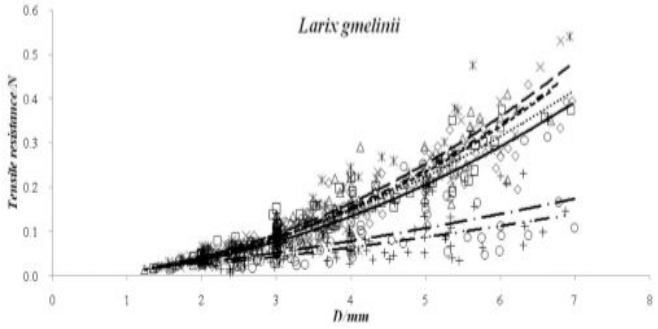

Figure 2.6: Effect of diameter on the tensile resistance of a plant species (after Yang et al, 2016)

EFFECT OF ROOT DIAMETER

The root diameter is an important mechanical aspect that influences the stability of slopes. Thin and fine roots provide tensile reinforcement to soils when the cross failure surfaces, contributing to the stability of the slope. Thick roots on the other hand act like soil nails on slopes, providing anchorage and reinforcing the soil. Yang et al (2016) studied the influence of the combined effect of root diameter and moisture content on the tensile properties by testing four different plant species. It was found that the root

diameter and root moisture had a strong effect on tensile resistance. Roots with larger diameter were found to have a higher tensile strength. Roots with a higher moisture content were observed to have higher tensile strength when compared to air dried roots (Yang et al, 2016).

EFFECT OF ROOT AREA RATIO

Genet et al (2008) conducted tests in Japan using the Japanese Cedar tree to understand the influence of spatial position of trees and stand age on the factor of safety of slopes. It was observed that mature plants, which have a high root density increased the apparent cohesion of the soil. The increase in cohesion was observed to be the highest in the upper half where the root area was higher and decreased gradually with depth.

EFFECT OF PLANTING PATTERNS

Fan, Chia-Cheng and Lai (2014) studied the effects of planting patterns on slope stability. The tests were conducted using two different planting patterns (uniform and alternating planting patterns) where the space between the plants were varied. It was observed that increasing the space between plants lead to the reduction of the FS of the slope. The increase in spacing between plants lead to the reduction in root area reinforcing the slopes.

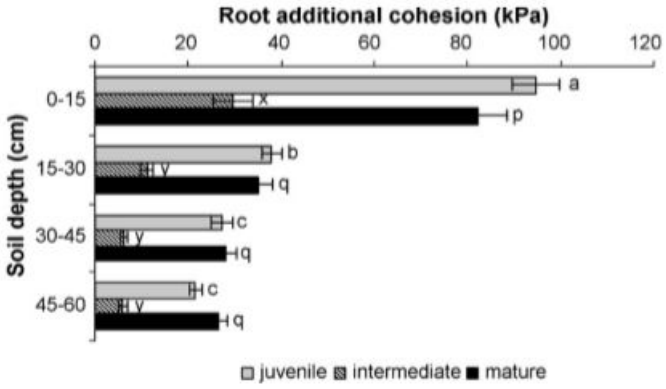

Figure 2.7: Effect of root area on the apparent cohesion of the soil (Genet et al, 2008)

2.4.2. ROOT REINFORCEMENT MODELS

The contribution of the root area to the increase in cohesion of the soil was quantified using two different models, namely the Root reinforcement model and the Dynamic Fibre Bundle model.

PERPENDICULAR MODEL

Researchers (Wu and Sidle, 1995; Waldron and Dakesian, 1981; Greenwood et al, 2004) suggested the addition of an apparent cohesion term to the Mohr-Coulomb equation, to model the influence of vegetation. The cohesion increase was calculated using the root reinforcement model developed by Wu et al (1979). The root reinforcement model is

based on the Mohr coulomb equation for calculating soil shear strength, which is given by the equation

$$S = c + \sigma_N tan\phi \tag{2.5}$$

where,
S is the shear strength of the soil,
c is the cohesion of the soil,
ϕ is the friction angle of the soil.
Endo T and Tsuruta (1969) observed that the friction angle of the bare soil and rooted soil remained the same. Wu et al (1976) formulated that the increase in shear strength of the soil is provided by the roots, which was given by the formula,

$$S_r = t_r(cos\theta tan\phi + sin\theta) \tag{2.6}$$

thus modifying the Mohr-coulomb equation to

$$S = c + \sigma_N tan\phi + S_r \tag{2.7}$$

Gray (1974) noted that the angle of internal friction was not affected by the presence of the roots in the soil, while Wu et al (1979) found through sensitivity analyses that the bracket term in (2.6) was not affected by variations in θ and ϕ. Hence the bracket term was assigned a constant value of 1.2. Thus, the simplified equation is given by,

$$S_r = 1.2 \sum_{i=1}^{n} \frac{n_i A_i}{A} * T_i \tag{2.8}$$

where,
1.2 is a constant which is a function of the friction angle and the angle of shear distortion between the root and the soil,
n_i is the number of roots in a defined area,
A_i is the area of the roots,
A is the area of the soil,
T_i is the Tensile strength of the root.
The root reinforcement model is based on a list of assumptions.

1. The roots are perpendicular to the slip plane.
2. The full tensile strength of all the root elements is mobilized when the soil shears.
3. It is assumed that the roots are well anchored and do not pull out when tensioned.

DYNAMIC FIBER BUNDLE MODEL

The Fibre Bundle Model(FBM) was developed to understand the behaviour of composite materials. The first model was developed by Daniels (1945). The FBM is based on the principle that the maximum load withstood by the bundle of fibers is less than the sum of each of their individual strengths. This is because , when the fibre bundle is loaded, not all the fibres break at the same time. On this assumption, two FBMs were developed by Hidalgo et al (2002), namely the Global Load Sharing system (GLS) and the Local Load

Sharing system (LLS) . The GLS model assumes that the load from the broken fibres is distributed evenly among the remaining intact fibres depending on their diameters . The interactions in the GLS system is hence assumed to be long range. The LLS system on the other hand assumes that the load from the broken fibres is redistributed from the broken fibres to the intact fibres based on the proximity of the broken fibres from the intact fibres. This mode of interaction is hence termed short-range interaction. The assumptions made in the FBM are,

1. The elastic properties of the fibres are the same
2. The roots are oriented parallel to each other and the direction of loading.

3

PHYSICAL MODELLING - DEVELOPMENT AND TESTING

3.1. INTRODUCTION

PHysical modelling, as defined by the Technical committee of the International Society of Soil Mechanics and Geotechnical Engineering (ISSMGE) is "a simplified physical representation of a finite boundary problem for which similarity is sought in the context of scaling laws". In layman's terms, physical modelling is a technique where scaled down versions of a prototype are built, to study the behaviour expected of a prototype. While it is possible to replicate the features of the prototype in a full-scale test, such tests are expensive, time consuming and offer limited control over the testing conditions. Physical models provide an advantage over field scale tests in terms of controlled conditions, also allowing for better visualization of the problem and validation of the numerical model (Shiau et al, 2016). The first physical model in geomechanics was developed by Terzaghi in 1936, which involved a simple device to model ground movements and to investigate the arching phenomenon.

Centrifuge modelling is a form of physical modelling where in-situ stress states observed in a full scale model are replicated in a scaled down model by subjecting the model to increased gravitational accelerations. The dimensions of centrifuge models are designed with the help of scaling laws, which help to design a scaled down version of a prototype, which when subjected to higher gravitational accelerations reproduces the stress states expected in the prototype. This helps researchers replicate conditions in the scaled down version, which may take much longer in the prototype.

Centrifuge modelling has been employed by researchers in the past to study the effect of vegetation on slope stability(Sonnenberg et al, 2010; Sonnenberg et al, 2012; Eab et al, 2014; Liang et al, 2015). The drawback of using vegetation in the centrifuge model, as reported by the researchers (Mickovski et al, 2009) is the modelling of root diameter using scaling laws, which leads to the over-estimation of the tensile strength of the roots. Repetition of tests is a another concern in the physical modelling of vegetated slopes, due to

the high variability in the architecture and mechanical properties of roots. Nevertheless, attempts have been made to understand the influence of vegetation on improving slope stability. To overcome the difficulty in the repetition of tests, model root analogues were used instead of live plants (Sonnenberg et al, 2012; Liang et al, 2015).
This chapter discusses the development of a 1g physical model of a sheet pile-vegetation system, to protect stream banks. Model root analogues having root architecture similar to *Humulus lupulus* L. were 3D printed to be used as reinforcement in the model stream bank. Results of three tests, one on bare soil and two using root analogues are reported in this chapter.

3.2. MATERIALS AND METHODS

SOIL CLASSIFICATION

The particle size distribution of the soil is presented in figure 3.1. Wet sieve analysis test on the soil showed a fines content of 18.56 %. Based on the particle size distribution, the soil was classified as silty sand (SM) under the USCS classification.

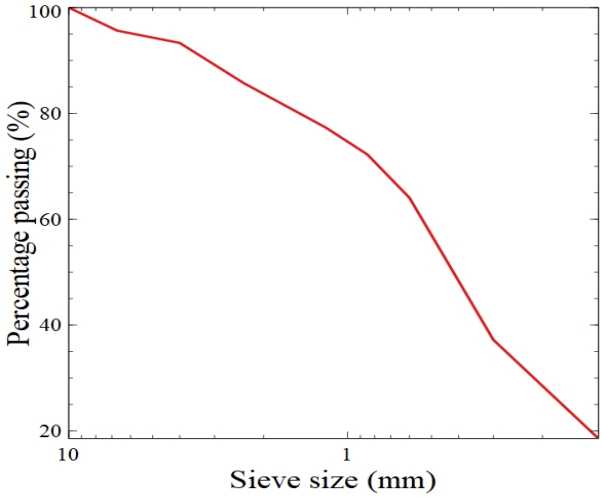

Figure 3.1: Particle size distribution of the soil used in this study.

DIRECT SHEAR TESTS

The shear strength properties of the soil were examined through standard direct shear tests on the samples. Three direct shear tests were performed and the soil samples for these three tests were prepared at a bulk density of 1.4 g/cc. The specimens were saturated before testing. The samples were sheared at a rate of 0.2 mm/min. The samples were tested under three different normal stresses of 22 kPa, 31 kPa and 47 kPa. The results of the tests are presented in figure 3.2.

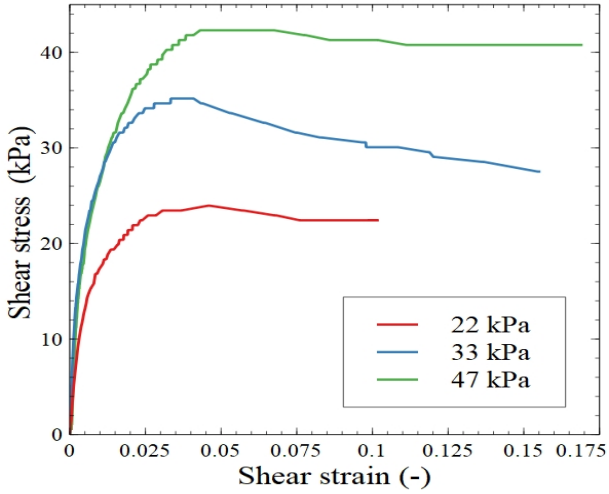

Figure 3.2: Shear stress vs shear strain of direct shear tests.

The soil showed a friction angle of 39 degrees. The dilatancy angle was derived from the plot of volumetric strain (eps1) versus shear strain (eps3),presented in figure 3.3. The dilatancy anles obtained for 22 kPa, 31 kPa and 47 kPa were 5^0, 7.5^0 and 1.3^0 respectively.

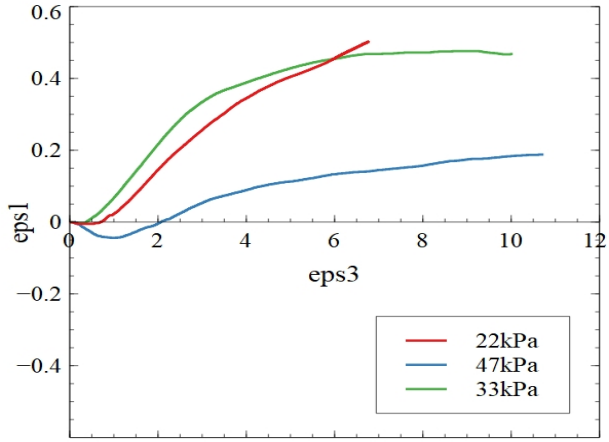

Figure 3.3: Volumetric strain(eps1) vs shear strain (eps 3).

TRIAXIAL TEST

Consolidated undrained triaxial tests were performed on the soil samples at confining pressures of 12 kPa. The soil samples were prepared at a bulk density of 1.4 g/cc.

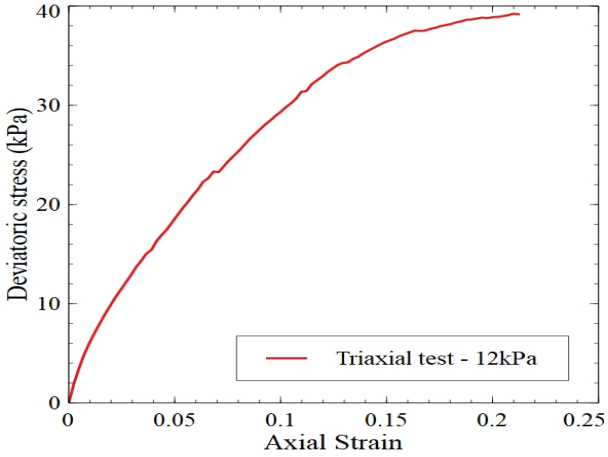

Figure 3.4: Deviatoric stress vs axial strain of triaxial tests.

The samples showed a peak strength of 40 kPa at the confining pressure of 12 kPa. The Young's modulus of the specimen was estimated to be 800 kPa.

3.2.1. PHYSICAL MODEL SETUP AND INSTRUMENTATION

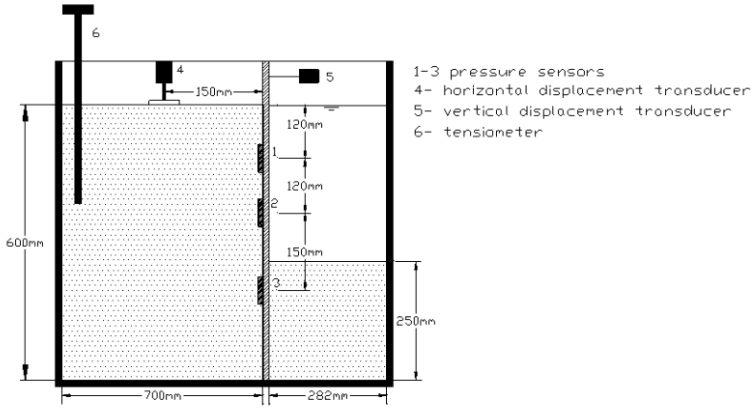

Figure 3.5: Pictorial representation of the model setup.

The test box had dimensions of 1000mm*700mm*700mm (figure 3.5). The box is made of plexwood of thickness 18mm. Additional vertical members were provided, to stiffen the box and to prevent any lateral deformations. One face of the box is made of fibre glass. This was done to use PIV to capture images of the failure surface. A PVC sheet

4mm thick is placed at the base of the box. This plate is lined with rubber strips along the edge to prevent the leakage of water.
A plexwood board 18mm thick, made of birch-wood is used as sheet pile. The board has a height of 700mm and a width of 695mm. Rubber linings are placed along the edge of the board to prevent the leakage of water when the model embankment is saturated.
Pressure sensors are placed along the inside of the wooden sheetpile to measure the pressure exerted by the soil mass and the water column. Displacement sensors are hooked to the outside of the sheetpile to measure the horizontal displacement of the sheetpile. A displacement transducer is placed on the top of the embankment to measure the settlements in the soil. A tensiometer is placed in the soil to monitor the suction in the soil and to ensure that the embankment is completely saturated. The sensors used in the test are listed in table 3.1. A Pentax k-70 DSLR camera is used to capture the development of the failure of the soil-sheetpile system. The setup is visualized below in figure 3.5.

Series	Manufacturer	Physical variable
MPXHZ6130AC6U	Farnel BV	Pressure
FDMK30	Althen BV	Displacement
13FLP	Althen BV	Displacement

Table 3.1: Type of sensors used in the test.

MPXHZ6130AC6U PRESSURE SENSORS

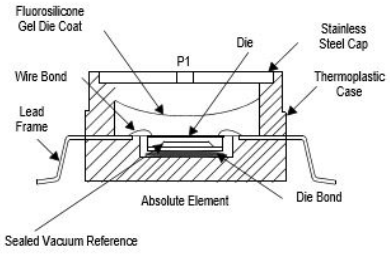

Figure 3.6: Cross-section of the sensor.

MPXHZ6130AC6U piezoresistive transducer manufactured by Premier Farnell Ltd., is a state of the art single conditioned silicon pressure sensor. This sensor combines advanced micro-machining techniques, thin film metallization, and bipolar semiconductor processing to provide an accurate, high level analog output signal that is proportional to applied pressure. These sensors are commonly used in altimeters, in engine manifolds and in weather stations to measure pressure. The cross-section of the sensor is presented in figure 3.6. The sensor is placed in a casing made of pvc and the casing is filled with silicon oil which acts as the medium for transferring the applied pressure to the sensor.

Figure 3.7: The PVC casing in which the sensor is placed.

The sensor has an output voltage of 5 volts and a pressure range of 130 kPa hence measuring 26 kPa per volt which is the correction factor. The sensor as a minimum range of 0.1 kPa. The pressure is caculated using the formula,

$$Reading = Voltage * Correctionfactor + Offset \tag{3.1}$$

This sensor is an absolute sensor which can also measure air pressure. Hence the ambient air pressure is entered as a negative offset value, which is automatically subtracted from the output.

FDMK30 ANALOG SENSOR

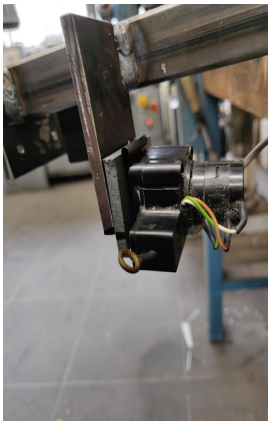

(a)

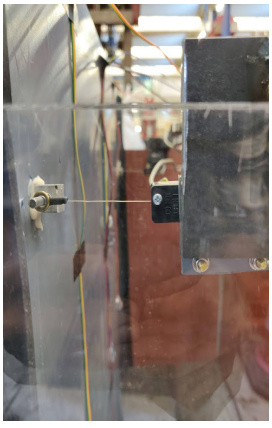

(b)

Figure 3.8: FMDK30 displacement sensor

The FDMK30 analog sensor is a draw wire sensor that is used to measure displacements. The sensor, manufactured by Althen Sensors BV, has a measuring range of 0.25 - 50 mm

and a supply voltage of 5 volts. The sensor is mounted on a custom made rail and the draw wire is hooked to the sheetpile to measure the movement of the sheetpile.

13FLP POTENTIOMETER

Figure 3.9: Vertical displacement sensor.

A linear variable differential transformer is installed on the back-fill at a distance of 15 cms from the sheetpile to measure the settlement or heave experienced by the embankment. The sensor was manufactured by Althen Sensors and Controls BV. This is a spring return type LVDT which is kept in constant contact with the soil. This allows the instrument to accurately measure any upward and downward vertical movement.The tip of the measuring rod is placed on a PVC sheet 3mm thick to prevent the LVDT from penetrating the soil. The instrument has a measuring range of 50mm.

PARTICLE IMAGE VELOCIMETRY

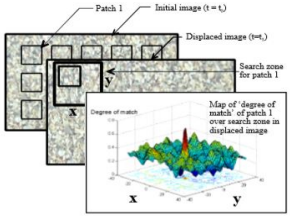

Figure 3.10: PIV image analysis technique (White et al, 2001)

Particle Image Velocimetry was originally developed in the field of fluid mechanics. The flow field of the fluid can be examined by seeding the flow with marker particles and tracking the movement of small patches within a larger image (Adrian, 1991). GEOPIV-RG is the set of image processing algorithms which were used to implement the patch matching technique used in the PIV method. To implement this, a grid of patches is

laid over the entire dimension of the embankment. The control points were placed at a distance of 5cm from each other over a dimension of 700 mm*500 mm. The patches are bounded by a predefined search zone. Each patch is translated at 1-pixel intervals and at each position, the degree of match between the sample patch and an interrogation patch taken from the same location in the subsequent image is assessed (White et al, 2001).

Figure 3.11: Pentax k-70 camera used for image acquisition

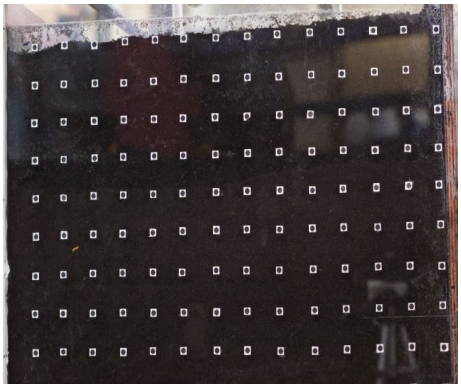

(a) Control points fixed on the model.

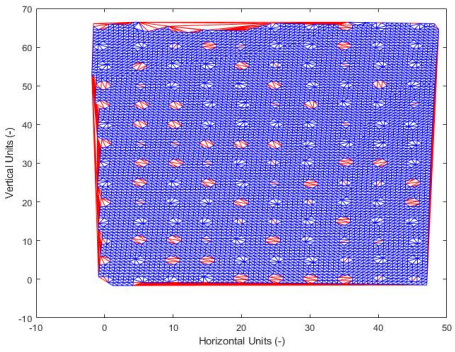

(b) Equivalent mesh.

Figure 3.12: Mesh generation based on the input of control points in the algorithm.

The images were shot on a Pentax k-70 DSLR camera. The images were shot continuously at a rate of 3 frames per second. The images were shot at a resolution of 6000*4000 pixels. The camera was controlled using a remote control once the camera position was fixed. A set of LED lights were used to brighten the cross sectional view of the embankment and to reduce the reflections on the fibre glass face.
The images captured are used to measure the displacements and strain in the system. Reference points are marked on an initial "reference image" which conform to pixel po-

sitions. Displacements are then calculated using the differences in the pixel positions in the subsequent images. Translations in pixels are converted into real time displacements of the soil particles in the reference area.
The reference image is converted into a mesh (figure 3.12(b)), which is used to measure the displacements and the strains in the system. The mesh is a set of strain elements that are created using Delaunay triangulation method. The red elements are invalid elements that are excluded from the computation.

3.3. ROOT ANALOGUE MODELLING

The 3-D root model used in this study was designed based on the root architecture of the *Humulus lupulus* L. plant reported by Graf et al (2014) and specimens grown in the botanical garden by a fellow PhD researcher*(personal communication). Three types of roots for the *Humulus lupulus* L. plant, based on its age:

1. Perennial woody roots that grow shallow out of the root-stock.

2. Fine young white roots growing out of the perennial roots.

3. Root developing out of the shoots above the root-stock.

Each section of the root system was approximated into different shapes. The vertical roots of the plant was cuboid shaped while the horizontal roots formed a cylinder shape around the root stock. The young white roots at the top of the section (row section) form a hilled up zone. The morphological root development of the *Humulus lupulus L.* plant is presented below. The root analogue used in this study is modelled in AutoCAD

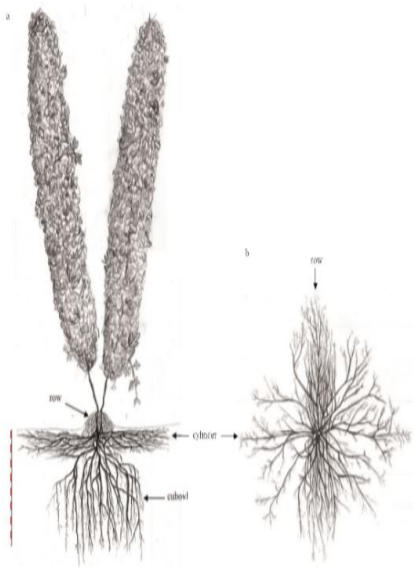

Figure 3.13: The root morphology of the humulus lupulus plant (Graph et al. (2014).

with simple extrusion techniques of cylinder shapes. The root model has a height of 250 mm and a diameter of 200 mm. The main tap root has a diameter of 20 mm. The average root diameter and the root area of each section is presented below. The row section of the root had to be omitted from the root model as the 3-D printer has a minimum spool diameter of 1 mm and hence cannot print parts less than 1 mm in diameter

Section	Average diameter(mm)	Root ratio (mm2)
Row	20	314
Cylinder	1.47	310
Cuboid	0.9	156

Table 3.2: Root diameter and root area of each section.

3.3.1. FABRICATION

The root modelled in AutoCAD is converted to an STL file (stereolithography), which is the standard file format used to for rapid prototyping and 3-D printing. The root is printed using the Ultimaker 3 , a 3-D printer manufactured by Ultimaker BV, a company based in The Netherlands. The printer works by printing an initial support structure on which the root model is printed. The support structure is printed at a lower density than the main model, and can be broken off. The models are printed on a hot plate of dimensions 200 mm * 200 mm. This limits the size of the models that can be printed in them. Hence the root model is printed into two halves. The minimum diameter of the spool that can be printed is 1 mm, which limits the printing of segments used to model fine roots. fine elements had to be omitted due to the difficulty in breaking from the support structure.

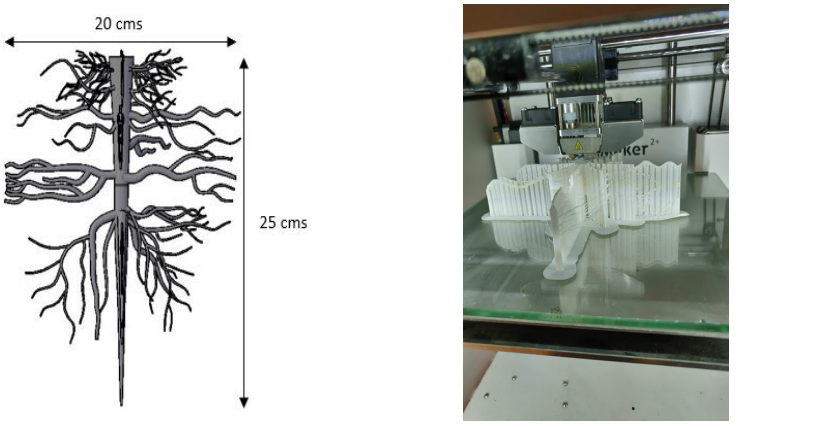

(a) AutoCAD root model of the *Humulus lupulus L.* .

(b) Root model printed on the support structure.

Figure 3.14: Design and fabrication of root elements.

3.4. DEVELOPMENT OF THE PHYSICAL MODEL

A preliminary investigation was conducted to arrive at the design of the physical model.The final model was developed by testing different model dimensions and materials.

3.4.1. PRELIMINARY TEST 1

The embankment in this model had the dimensions 700mm*700mm*600mm, with a retaining height of 320mm and an embedment depth of 280mm. The sheetpile used in this model was a PVC sheet of thickness 8mm, breadth of 700mm and a height of 700mm. Rubber linings were provided along the edge of the sheetpile and was placed in contact with the walls of the test box. This was done to prevent the flow of water from the embankment into the river side of the test box. Petroleum jelly was applied on the area of the side walls that came in contact with the rubber linings, to reduce the friction between the rubber lining and the glass wall. The testing protocol adopted for the test is given in section 3.4.2.

Figure 3.15: PVC sheetpile with sensors attached.

3.4.2. TESTING PROTOCOL

1. A tensiometer was placed in the embankment to measure the suction in the soil. The tensiometer is placed at a distance of 500 mm from the sheetpile.

2. Water was filled up to the top on the passive side (river side) of the system.

3. Once water was filled on the passive side, the embankment was saturated. The setup was kept undisturbed for 24 hours to make sure the embankment saturates completely. The suction was monitored throughout the filling process.

4. Once the embankment was saturated, water was pumped out of the passive side at a rate of 4.2 litres/min using a hand pump. The water was pumped out until the embankment collapsed.

5. The horizontal displacement of the sheetpile, vertical displacement of the embankment and the pressure on the sheetpile were monitored throughout the draw-down process.

6. The DSLR camera captured images of the embankment throughout the draw-down process.

RESULT

Difficulties were encountered during the model preparation, with the sheetpile tending to deflect during the tamping of the embankment. Extra reinforcement was provided in the form of wooden struts to prevent the deflection of the sheetpile. Though the embankment could be kept stable during the model preparation, the sheetpile was too thin to keep the embankment stable during the saturation procedure. As a result, the embankment failed during the initial preparation.

It was evident from the failure that the thickness of the sheetpile and the embedment depth were primary reasons for the instability. As a result, a thicker sheetpile and higher embedment depth was used.

3.4.3. PRELIMINARY TEST 2

To address the shortcomings of the model in preliminary test 1, a plexwood sheetpile of thickness 20mm was used. The same retaining height and the embedment depth of 320mm and 280mm, as in test model 1 , were adopted in this model. The sheetpile was again lined with rubber strips to prevent the flow of water from the embankment into the river side. The testing protocol followed in preliminary test 1 was adopted for this test.

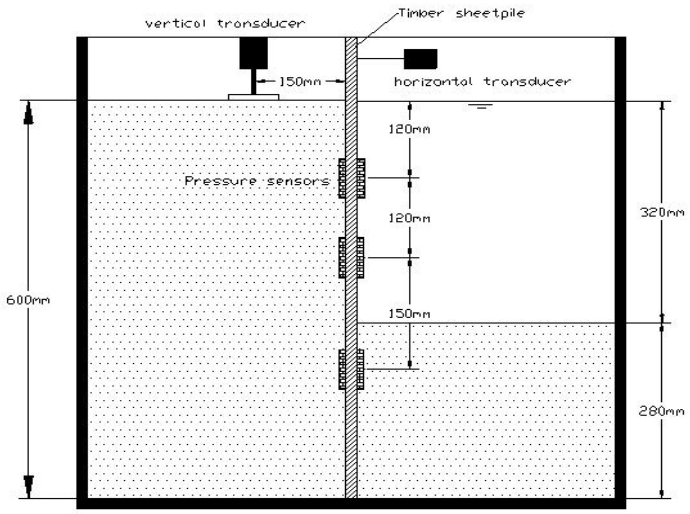

Figure 3.16: PVC sheetpile with sensors attached.

The horizontal displacement and vertical displacement of the soil was plotted against

the ratio (Rd/Dd), and is shown in the figures below. No significant vertical displacement was recorded till a Rd/Dd ratio of 0.2. There is almost a linear increase in vertical displacement with draw-down. A maximum vertical displacement of 6 mm was recorded at a draw-down ratio of 1. A maximum horizontal displacement of 10.5 mm was recorded. The failure wedge observed was a crack formed at a distance of 100mm from the sheet pile. While a crack was observed on the top of the soil, there was no observable failure in the system. The embankment remained stable for the entire draw-down condition.

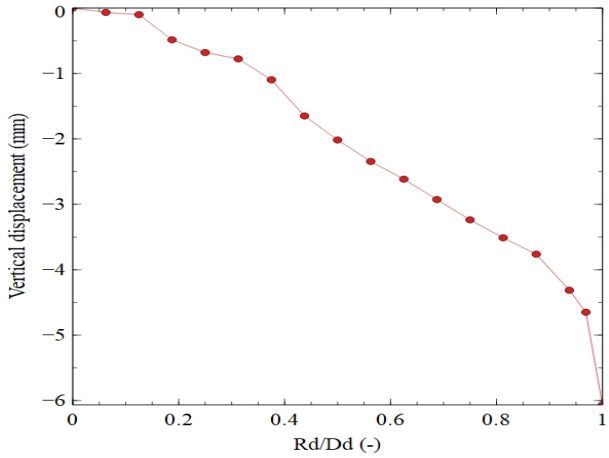

(a) Vertical displacement

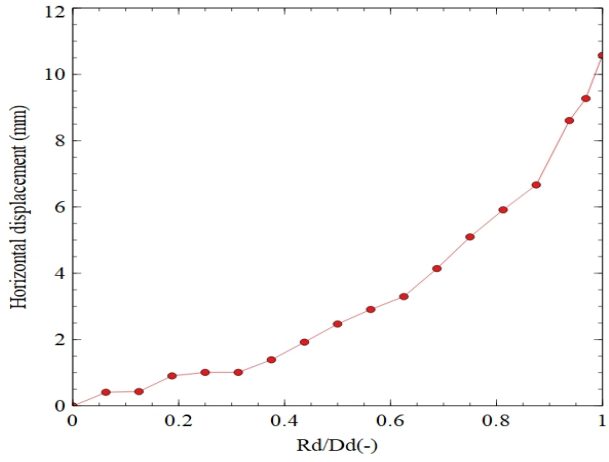

(b) Horizontal displacement

Figure 3.17: Vertical and horizontal displacements - test model 2

DISCUSSION

Using a thicker sheet-pile helped keep the embankment stable during the initial preparation. While the embankment did not experience failure for the entire draw-down condition, cracks were seen to have formed at the surface of the embankment. As the aim of

the test was to bring the embankment to complete failure, this result was not sufficient. As it was evident that the embankment was close to failure, the best course of action was to reduce the passive resistance by reducing the embedment depth of the sheetpile. This observation was addressed in the final model.

3.5. TESTING OF THE PHYSICAL MODEL

3.5.1. FINAL MODEL

Based on the results of the previous tests, the retaining height of the embankment was increased to 350mm and the embedment depth was decreased to 250mm. The model sheetpile with the sensors fixed on them are put in place before the filling process starts. The model embankment is 700mm * 700mm * 600mm and is prepared in three stages of 700mm * 700mm * 200mm at a dry density of 1.2 g/cc. Each layer is prepared by pouring in the sand using a bucket which is weighed with the sand. The sand is then manually compacted using a customized compaction rod of weight 10 kgs dropped from a height of 150 mm. After each layer is filled, the surface is scrapped with steel rod to ensure bonding between the next layer on top. The density of the each layer was checked after compaction by removing soil cores from the embankment. The sheetpile is given an em-

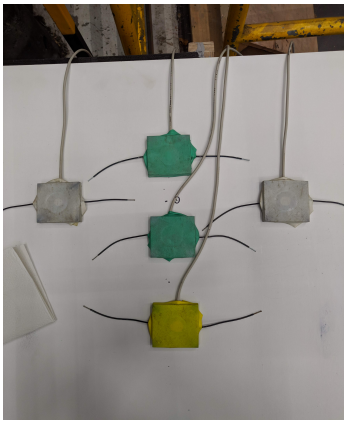

(a) Arrangement of the pressure sensors.

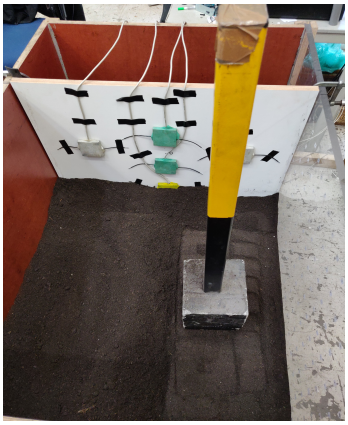

(b) Preparation of the slope - compaction.

Figure 3.18: Model setup

bedment depth of 250mm. The rubber linings on the sheetpile are placed in contact with the walls of the box to prevent water flowing between the back-fill and the embedment side. Petroleum jelly is applied on the area of the rubber lining that comes in contact with the walls of the container, to reduce the effects of friction between the rubber and the wooden/glass side walls. The top of the sheetpile is secured using clamps to restrain the sheetpile from moving while filling the soil.

Figure 3.19: Clamps used to restrain the sheetpile during filling.

3.5.2. ROOT INSTALLATION

Three different techniques were tested for the installation of the root analogues.

1. Pushing the root analogues into the soil.

2. Placing the root analogues in a soil slurry.

3. Excavating holes in the prepared embankment and installing the root analogues.

Pushing the root analogues into the soil was not successful as the root elements suffered damages. While it was easier to place the root elements in a soil slurry, achieving the required density in the soil after installation of the elements was a tedious process. The 3D root elements were finally installed by excavating the soil in the designated positions, after preparing the embankment. This technique ensured that the installation of the root elements did not affect the preparation of the embankment. Two tests were conducted with the roots placed in two different patterns and two different distances from the sheetpile, to observe the influence of the two planting patterns on the stability of the embankment.
Holes of 230 mm diameter and 250 mm depth were dug to place the root elements in the soil. In pattern 1, two roots were placed at a distance of 180 mm from the sheetpile and at a distance of 180 mm from each other. The third root was placed in a second row at a distance of 200 mm from the first row and in between the two roots. In pattern 2, the number of root elements was increased to 5, with three roots placed in the first row and two roots placed in the second row. The first row of roots were placed at a distance of 10 mm from the sheetpile with the main tap root at a distance of 110 mm from the sheetpile. The roots were placed at 30 mm spacing. The second row of roots were placed at a distance of 80 mm from the sheetpile with the tap roots at a distance of 180 mm from the sheetpile.

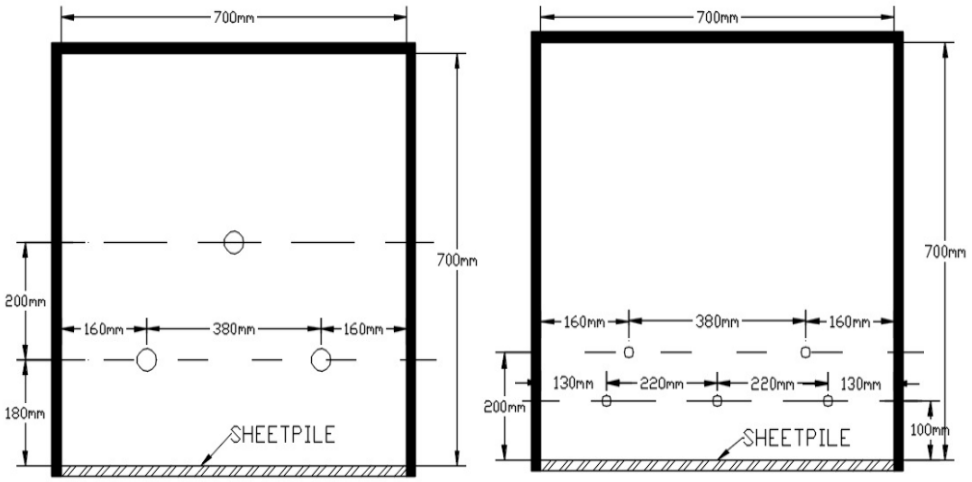

(a) Pattern 1.

(b) Pattern 2.

Figure 3.20: Planting pattern used in the experiments.

Once the roots were placed, the soil was pluviated into the hole in layers and compacted to the required density.The tamping was done manually using a small tamping device to ensure that the root elements were not damaged during the tamping process.

3.6. RESULTS AND DISCUSSIONS

3.6.1. BARE SOIL TEST

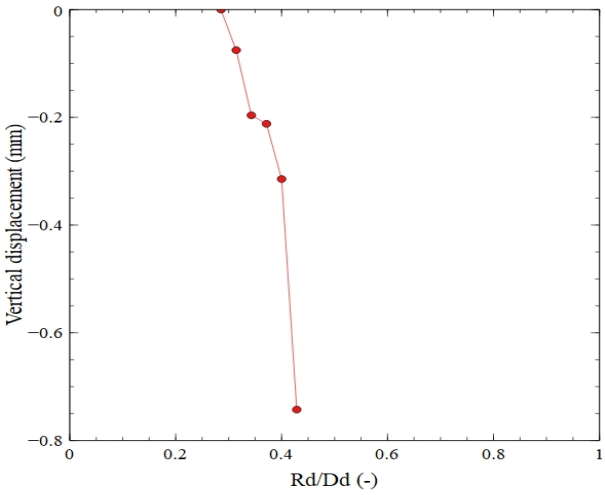

Figure 3.21: Vertical displacement

The vertical displacement, horizontal displacement and the development of pressure in the soil were plotted against the ratio of retaining height to the draw-down depth (Rd/Dd), and are shown in figures 3.21, 3.22 and figure 3.23 respectively. No settlement was observed in the embankment until a (Rd/Dd) ratio of 0.3, after which a settlement was initiated. The soil experienced a settlement of 0.75mm at a (Rd/Dd) ratio of 0.41. The soil experienced a horizontal displacement of 7.47 mm. The failure is triggered at a (Rd/Dd) ratio of 0.39. The maximum pressure recorded is 1.38 kPa.

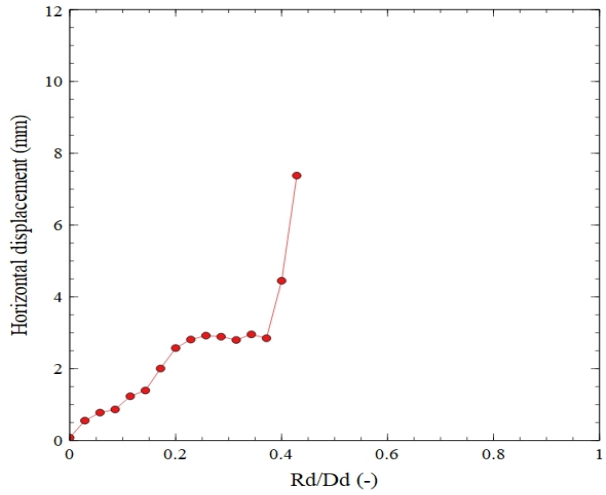

Figure 3.22: Horizontal displacement

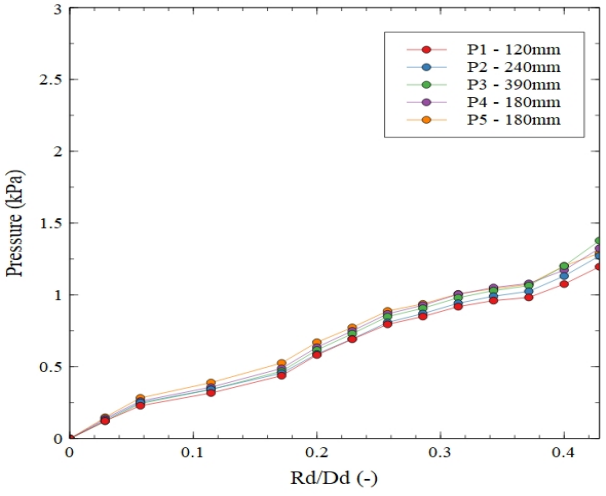

Figure 3.23: Horizontal displacement

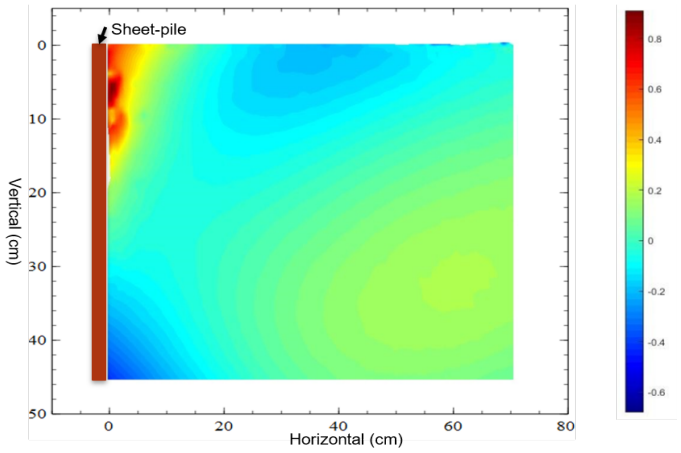

Figure 3.24: Horizontal displacement contour.

The failure wedge occurred at a distance of 100 mm from the sheetpile. The failure wedge was triangular in shape and extended to a depth of 200 mm. The failure occurred along the entire width of the embankment. The displacement vectors and the resultant contours obtained from the PIV analysis are presented in the figure 3.23. The displacement trend is extended over a width of 100 mm and to a depth of 250 mm. The displacement of the soil in the opposite direction between the depths 320 mm and 450 mm shows that the sheetpile experienced a rotational failure.

3.6.2. ROOTED SOIL TEST

PATTERN 1

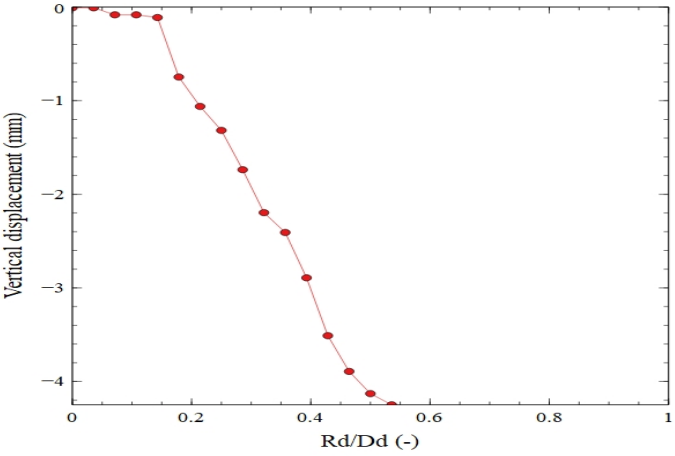

Figure 3.25: Settlement of the embankment vs drawdown depth.

The vertical displacement of the soil body vs drawdown depth is shown in figure 3.25. The horizontal displacement of the sheetpile is plotted against the drawdown depth and shown in figure 3.26. The development of pressure with drawdown depth for pattern 1 is shown in figure 3.27. The embankment experienced a settlement of 4.65 mm. The sheetpile experienced a horizontal displacement of 3.76 mm at an (Rd/Dd) ratio of 0.5 . The pattern shows a 50% decrease in displacement as compared to the bare soil model. The failure wedge was wider and deeper compared to the bare soil , extending along the entire width of the embankment.

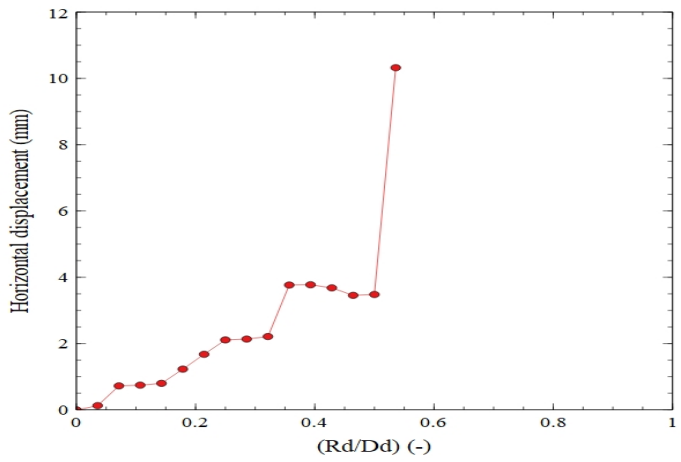

Figure 3.26: Horizontal displacement of the embankment vs draw-down depth.

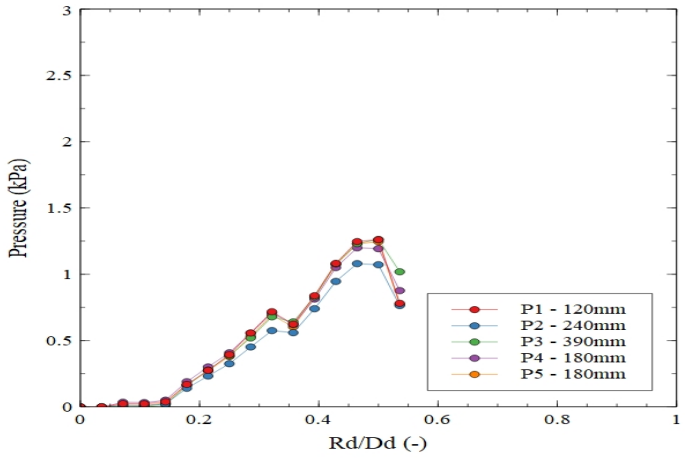

Figure 3.27: Pressure versus draw-down depth for pattern.

The active pressure exerted by the rooted embankment is less than the pressure exerted by the bare soil embankment. The maximum active pressure exerted is 1.08 kPa as

compared to the 1.61 kPa exerted in the bare soil model (at a depth of 390 mm) for the (Rd/Dd) ratio of 0.5. The failure wedge observed was 120 mm at the widest part in comparison to the 100 mm width observed in the bare soil embankment. The failure type observed here was a intact sliding block. The wedge extended to a depth of 300 mm. The vector displacements and the resultant contours of the root pattern 1 are shown below. The width of the failure wedge is measured to be 125 mm, which is 25 mm wider than the bare soil model. The failure wedge is observed to be deeper than the failure wedge observed in the bare soil model.

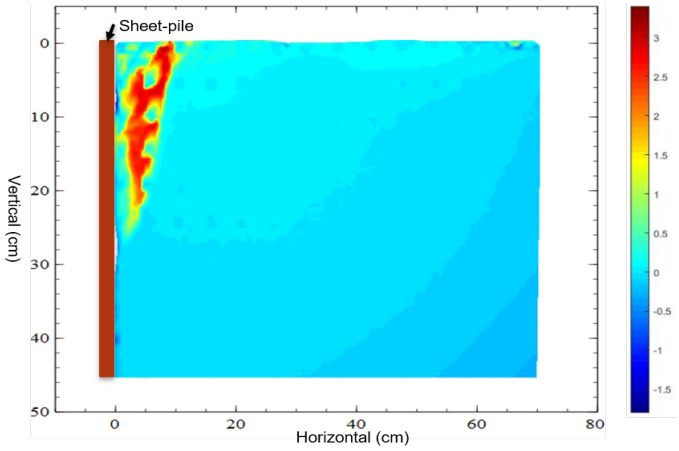

Figure 3.28: Horizontal displacement contours.

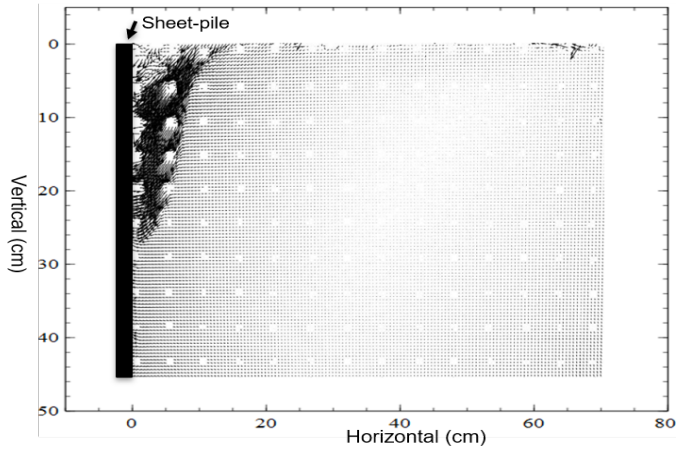

Figure 3.29: Resultant displacement contour.

PATTERN 2

The vertical settlement of the embankment is shown in figure 3.30. The horizontal displacement of the sheetpile is shown in figure 3.31. The development of pressure with draw-down depth is shown in figure 3.32. The soil body experienced a vertical displacement of 1.64 mm.

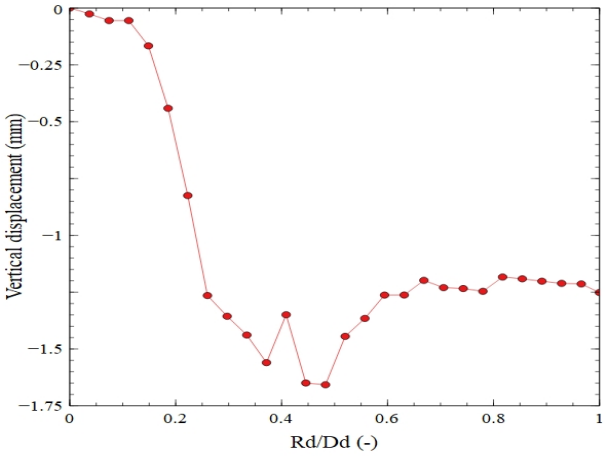

Figure 3.30: Settlement of the embankment vs drawdown depth.

The sheetpile experienced a horizontal displacement of 3.18 mm at an (Rd/Dd) ratio of 0.5. The displacement is 16% less compared to the first pattern where the root models were placed at a distance of 180 mm from the sheetpile. The maximum displacement experienced by the embankment was 3.5 mm. The embankment did not experience any further displacement with draw-down.

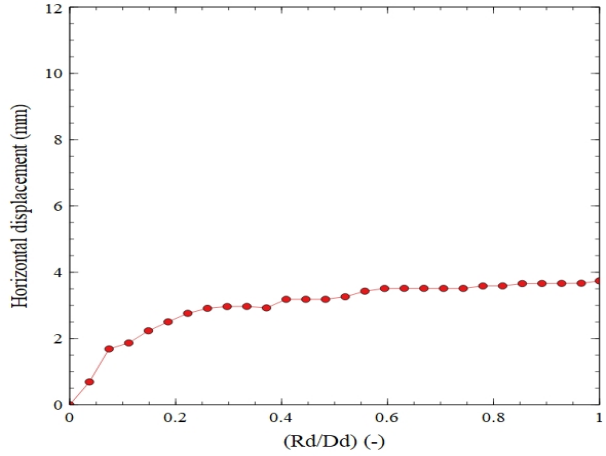

Figure 3.31: Horizontal displacement of the embankment vs drawdown depth.

The evolution of pressure with drawdown depth is shown below. The maximum pressure of 1.82 kPa was experienced at a depth of 180 mm for an (Rd/Dd) ratio of 0.7. The observed pressure was higher than what was recorded in the bare soil experiment and the pattern 1 of the rooted experiment as the embankment remained stable at a higher drawdown depth as compared to the bare soil test and root pattern 1.

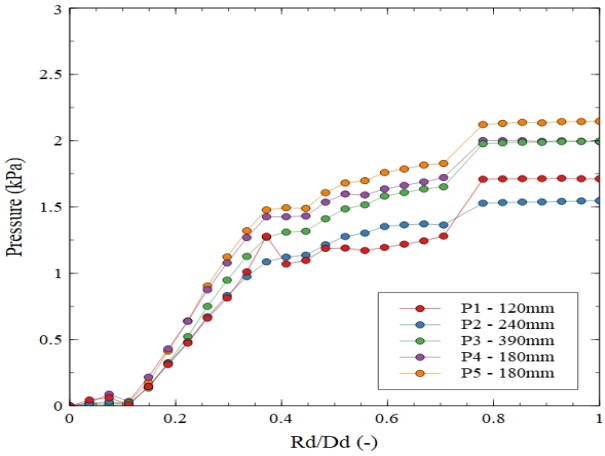

Figure 3.32: Plot of pressure vs drawdown depth for pattern 2.

It can be seen from the contours in figure 3.33 that the displacements in the rooted area is zero, except at the top. The embankment experienced a maximum horizontal displacement of 3.2mm at the top. The displacements are limited to the top of the embankment while the deeper sections were stabilized by the roots. The embankment remained stable without any further displacements with further draw-down of water.

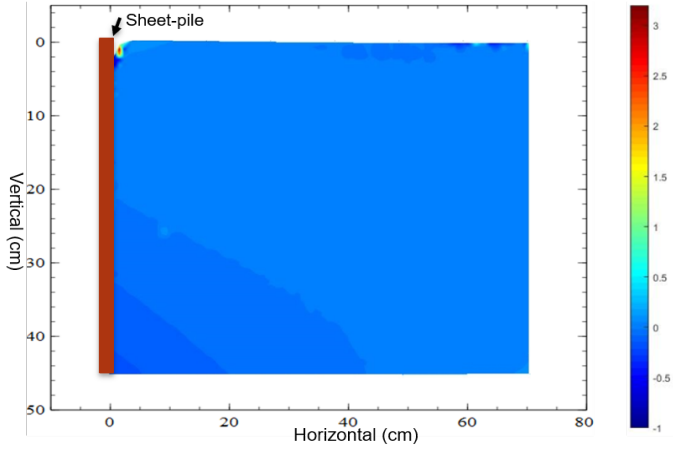

Figure 3.33: Horizontal displacement contours.

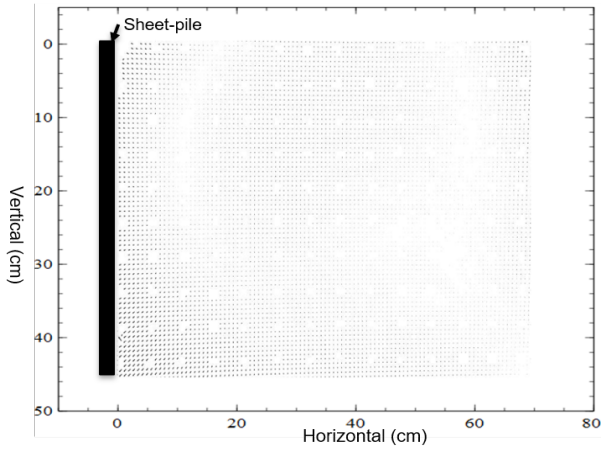

Figure 3.34: Vectorial displacements.

3.6.3. DISCUSSION

INFLUENCE OF MODEL ROOT ANALOGUES ON FAILURE PATTERN

The influence of the roots can be observed when comparing the behaviour of the bare soil model and the rooted models. The failure wedge in first rooted model (pattern 1), was observed to be wider and deeper compared to failure wedge in the bare soil model, implying that a larger volume of soil was mobilized. The presence of roots was identified to change the slope failure mechanism from a block failure to an intact sliding block (Sonnenberg et al, 2012). The presence of tree roots was found to improve the stability of a slope but accompanied by an increase in depth of slip surface (Kondo et al, 2004). When the embankment was 'heavily' reinforced in the second rooted model (pattern 2), the embankment remained stable at all draw-down depths. A higher initial displacement was observed for the sheet pile up to an (Rd/Dd) ratio of 0.34 in case of pattern 2, compared to pattern 1 and bare soil. This could be due to the additional displacement required to mobilize the tensile strength of the root analogues. A higher initial slope surface movement was reported by Askerinejad and Springman (2015) for vegetated slopes, in their centrifuge studies on rainfall induced landslides. The displacement trend of pattern 2 stabilized after an (Rd/Dd) ratio of 0.42 implying that sufficient root reinforcement was mobilized to stabilize the embankment. Comparing all the three cases, it can be concluded that,in the presence of roots, a higher volume of soil would have to be mobilized at failure, leading to a deeper and wider failure pattern.

INFLUENCE OF SPATIAL PATTERN OF ROOT REINFORCEMENT

The data obtained from the tests of pattern 1 and pattern 2 show that placing the roots closer to the sheetpile, at smaller spacing and within the influence zone, reinforces the embankment better than the wider spacing where the reinforcement provided within the influence zone is less. This also shows the effect of the extent of root reinforcement on the stability of the embankment. Fan et al (2014) reported that slopes with uniformly spaced planting patterns showed a factor of safety 3-4% lower than that of alternately

spaced planting patterns. A decrease in FS with an increase in spacing was also reported in the same study. A similar observation was made by Liang (2015) who suggested that the extent of lateral and vertical reinforcement provided by the vegetation system is more important than the increase in cohesion provided by the root system.

USE OF ARTIFICIAL ROOTS IN THE PLACE OF REAL ROOTS

It had been discussed earlier that the mechanical properties of the PLA material are similar to that of the root of *Humulus lupulus* L. plant. The results obtained in the tests, which were performed at 1g were comparable to the behavior of the systems where researchers used live plants in a centrifuge at higher g (Mickovski et al, 2009; Sonnenberg et al, 2012). Sonnenberg et al (2012) observed the presence of the root elements changed the failure system from block failure to an intact sliding block. The results of this experiment are also comparable to the results of Liang (2015), who used artificial root elements to study the seismic performance of vegetated slopes. The test was conducted at 10g in a centrifuge with the root dimensions modelled according to the scaling laws. Liang observed a reduction in displacement and settlements in rooted slopes when subjected to seismic motions (aftershocks).The comparable results suggest that artificial elements could be used as a substitute to live plants at 1g, which saves time and also improves the repetition of tests.

4

PLAXIS MODELLING

4.1. MODEL OVERVIEW

4.1.1. MODEL DIMENSIONS

THE dimensions of the physical model (embankment 700mm*700mm*600mm and retaining depth of 300mm*700mm*250mm) were replicated in the PLAXIS model. The PLAXIS model is shown in figure 4.1.

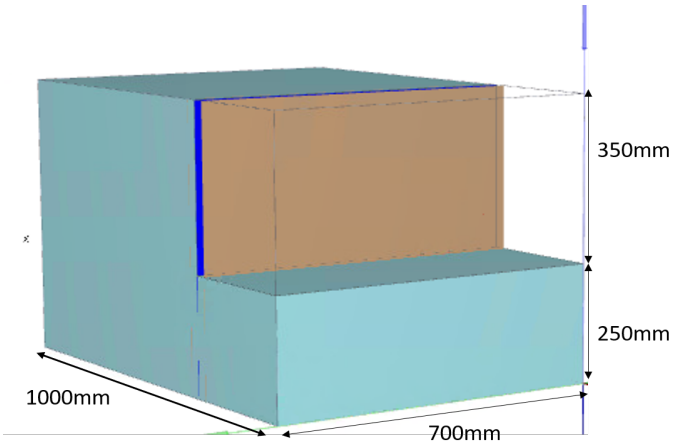

Figure 4.1: PLAXIS model dimensions

In PLAXIS 3D, the soil elements of the finite element mesh are 10-node tetrahedral elements. Plates are 6-node plate elements, which are used to model sheet piles. 12-node interface elements are used to model the soil-structure interaction.

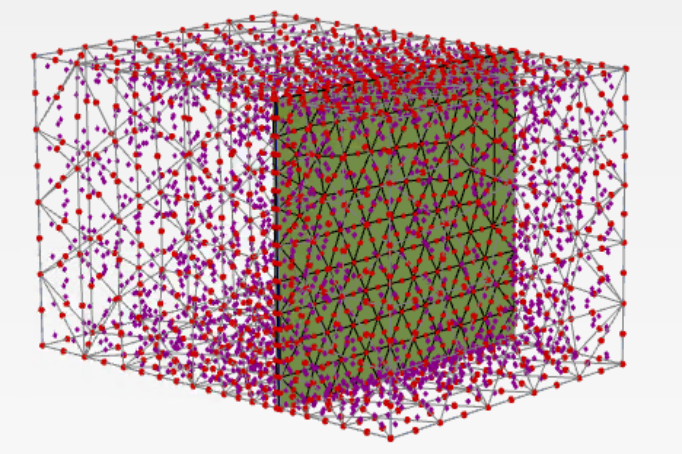

Figure 4.2: Element distribution of the model

4.1.2. BOUNDARY CONDITIONS

The outer boundaries of the model are closed to prevent the flow of water outside the model dimensions. The active in flow option is selected to make the sheetpile act as an impermeable boundary. The water level in the system is defined in two conditions. The water level in the passive side is defined at the height of the embankment at the initial stage and given drawdown conditions in later stages. The water level in the embankment is defined as constant for all drawdown phases.
The boundaries along the x-axis and y-axis ($x-min$, $x-max$ and $y-min$, $y-max$) were normally fixed, allowing lateral displacements. The lower boundary of the z-axis ($z-min$) is fully fixed, while the upper boundary ($z-max$) is free to allow lateral and vertical displacements.

4.1.3. MATERIAL PROPERTIES

The material properties of the soil and the sheetpile are summarized in table 4.1 and table 4.2. The soil is modelled using the Mohr-Coulomb model as this model is a reliable first approximation of the behaviour of soil. The input for the strength properties of the soil were based on the best fit for replicating the results obtained in the test on bare and rooted embankments. The sheetpile is defined as a plate and was assigned the mechanical properties of the birchwood sheetpile used in the experiment.

The testing procedure adopted in the simulation follows the testing protocol used for the experiment. The horizontal displacements, vertical displacements and the failure plane of the three models are compared with the data obtained from the experiments.

Parameter	Sign	Value	Unit
Material model	-	Mohr-Coulomb	-
Drainage type	-	Drained	-
Unit weight	γ	12	kN/m^3
Saturated unit weight	γ_s	15.55	kN/m^3
Effective Young's modulus	E'	1300	kN/m^2
Cohesion	C	0	kN/m^2
Friction angle	ϕ'	36	degrees
Dilatancy angle	ψ	0	degrees
Permeability	k	0.0002	m/min
Poisson's ratio	ν	0.26	-

Table 4.1: Input parameters for soil.

Parameter	Sign	Value	Unit
Thickness	d	0.018	m
Young's modulus	E	6*10^6	kN/m2
Poisson's ratio	ν	0.42	-
Specific weight	w	6.37	kN/m3

Table 4.2: Input parameters for sheetpile.

4.2. ROOTED SOIL MODEL

The reinforcement provided by the root was modelled in the form of a cohesion increase for the area covered by the root model. Each root element was modelled as a cuboid area of dimensions 200mm*200mm*250mm. Two different root placement patterns were used, similar to the patterns used in the experiment. The planting patterns are shown below in figures 4.3 and 4.4.

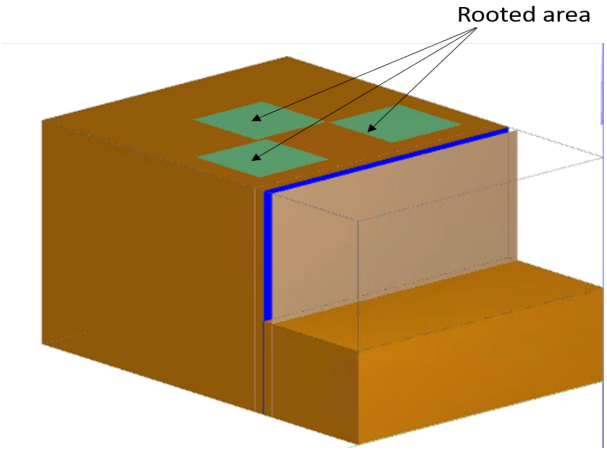

Figure 4.3: Root pattern 1

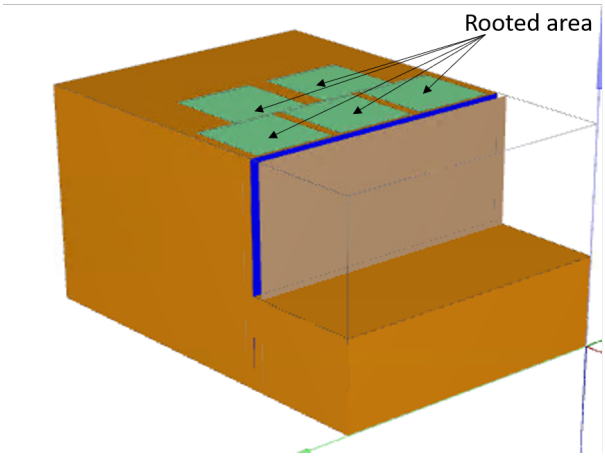

Figure 4.4: Root pattern 2

The properties of the rooted area are summarized below. The properties of the soil is similar to the bare soil model.

Parameter	Sign	Value	Unit
Material model	-	Mohr-Coulomb	-
Drainage type	-	Drained	-
Unit weight	γ	12	kN/m^3
Saturated unit weight	γ_s	15.55	kN/m^3
Effective Young's modulus	E'	1300	kN/m^2
Cohesion	C	7.6	kN/m^2
Friction angle	ϕ'	38	degrees
Dilatancy angle	ψ	0	degrees
Permeability	k	0.0002	m/min
Poisson's ratio	ν	0.26	-

Table 4.3: Input parameters for rooted area.

4.2.1. RESULTS

The horizontal and vertical displacements of the soil body in the three models are presented in figures 4.5, 4.6 and 4.7.

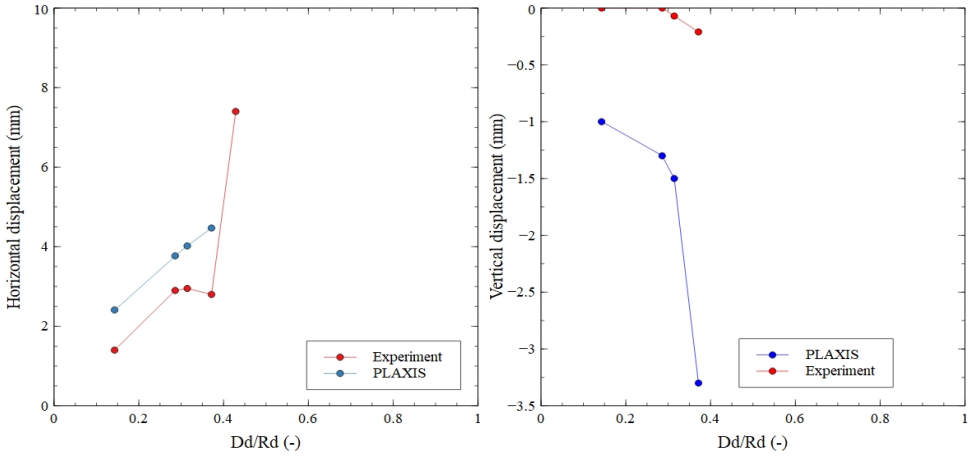

(a) Horizontal displacement (b) Vertical displacement

Figure 4.5: Bare soil model.

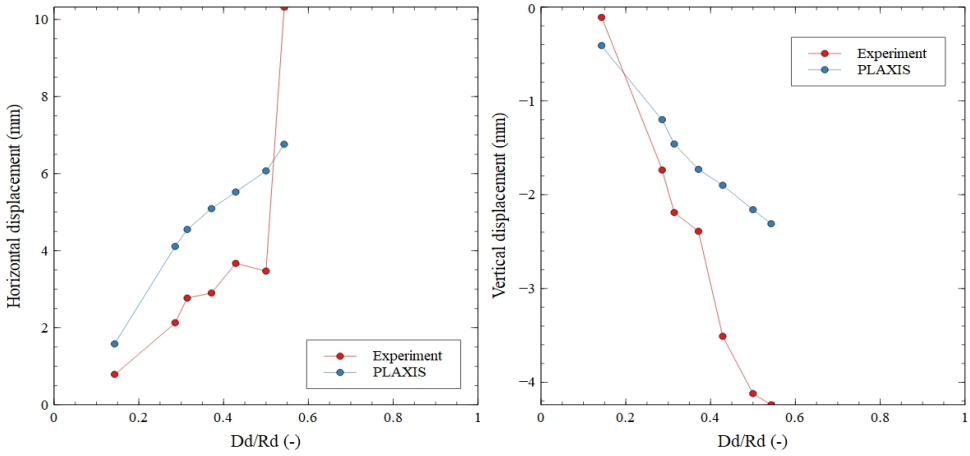

(a) Horizontal displacement. (b) Vertical displacement.

Figure 4.6: Root pattern 1.

The reduction in horizontal and vertical displacements observed in the experiment in the presence of the root systems was also observed in the PLAXIS model. The graphs show that the presence of the root systems stabilized the models at higher drawdown depths. The PLAXIS bare soil model failed at a Dd/Rd ratio of 0.4 and at a Dd/Rd ra-

tio of 0.5 in the root pattern 1 model, which were the same points at which failure was observed in the bare soil and root pattern 1 experiments. While the displacements captured in the PLAXIS model are higher than the displacements observed in the experiment, the displacement trends are similar. The higher displacement can be explained by the stiffness assumed in PLAXIS. The Mohr-Coulomb model assumes a constant average stiffness throughout the layer and does not take unloading stiffness into account. The model assumes a constant stiffness in points in the model at depths where the stiffness is higher due to higher confining stresses. Hence higher lateral displacements are observed. The assumption of constant average stiffness also leads to the under-prediction of settlements during as lower stiffness leads to the over-prediction of heave. These observations were reported by Hsiung et al (2014) when modelling the deflections of sheet-piles during excavations in sands.

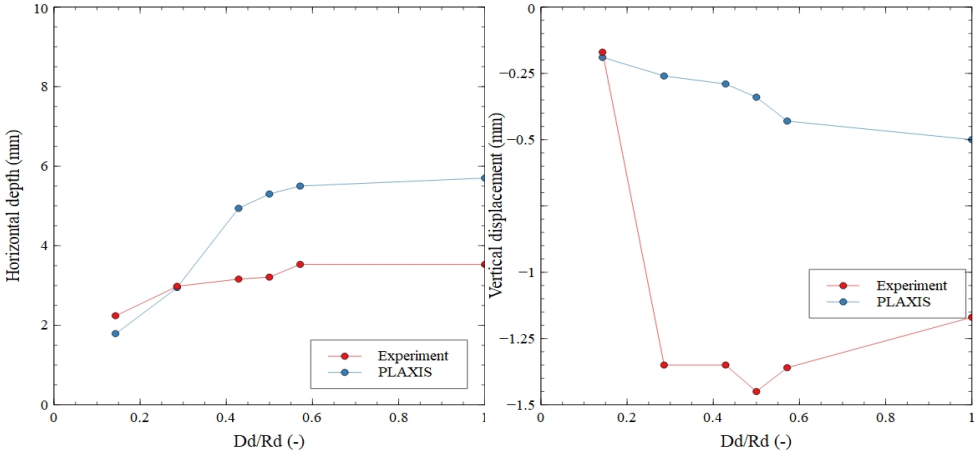

(a) Horizontal displacement.

(b) Vertical displacement.

Figure 4.7: Root pattern 2.

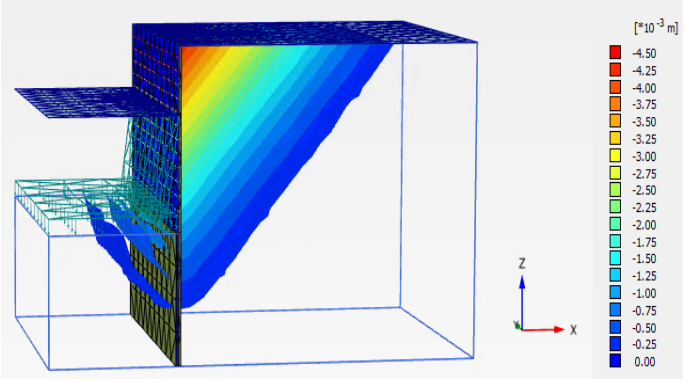

Figure 4.8: Failure surface observed in the model.

The failure pattern observed in the model is shown in figure 4.8. The failure pattern follows the triangular wedge observed in the experiment. The zone of influence observed in the PLAXIS model is larger than the zone of influence in the experiment.

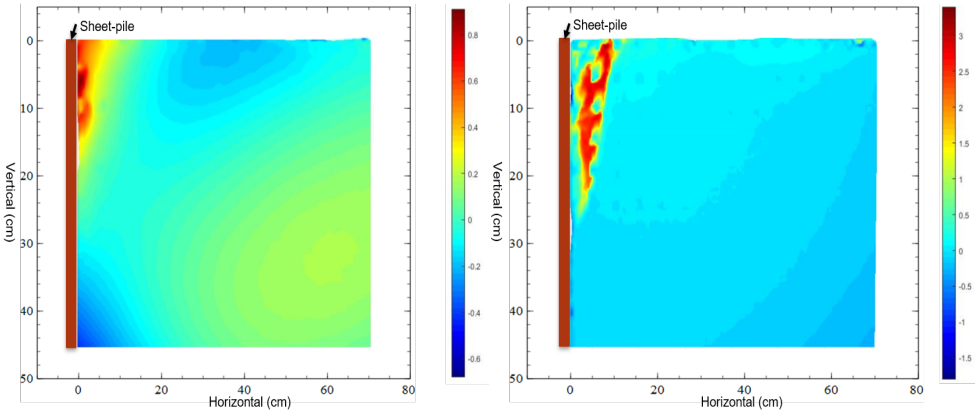

(a) Bare soil.

(b) Root pattern 1.

Figure 4.9: PIV contours - Horizontal displacement.

The effect of the rooted elements can be seen from the reduced displacements in the embankment.The failure pattern of the rooted model is wider, as was observed in the experiment. The maximum displacement is seen at the tip of the embankment. As observed before , the influence zone is wider than the influence zone observed in the experiment.

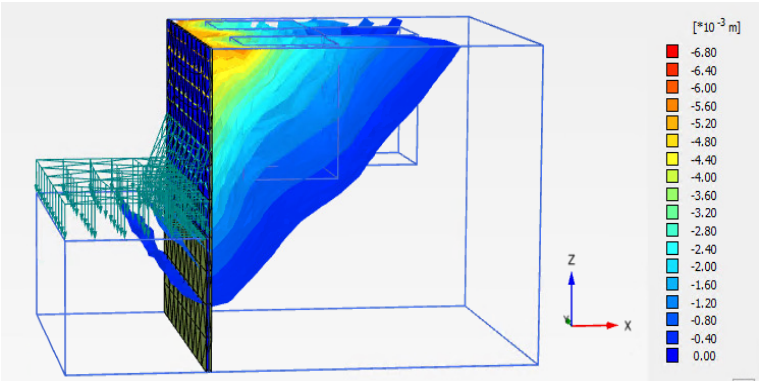

Figure 4.10: The displacement pattern observed in root pattern 1.

In root pattern 2 , the displacements closer to the sheetpile are less, compared to root pattern 1 , where the roots were placed further away from the sheetpile. The displacement along the entire width of the embankment was reduced more than in the case of

root pattern 1. The vertical displacement in this root pattern is less than root pattern 1. This shows the effect of root area in stabilizing the embankment.

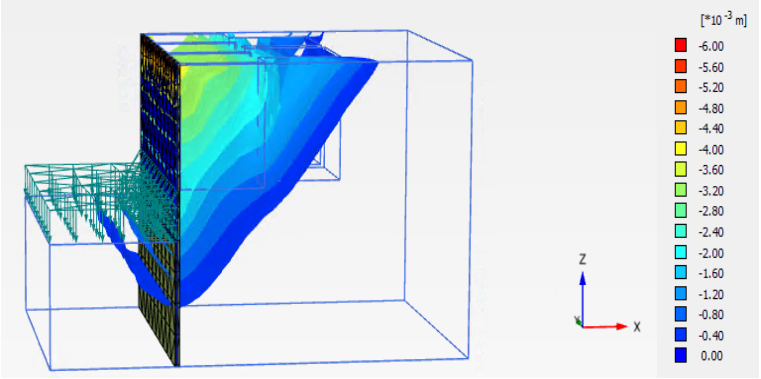

Figure 4.11: Displacement contour observed for root pattern 2.

The presence of the increased root area closer to the sheetpile reduced the displacements near the sheetpile thereby stabilizing the embankment for the entire draw-down condition. The influence zone observed in PLAXIS is larger than what was observed in the experiment.

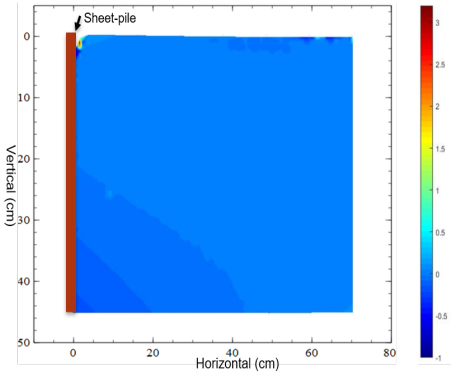

Figure 4.12: Displacement contour observed for root pattern 2 in the experiment.

4.3. DISCUSSION

ARE PLAXIS RESULTS COMPARABLE TO THE EXPERIMENTS

The bare soil model captures a triangular wedge-shaped failure plane which is similar to the failure wedge that was observed in the PIV contours of the bare soil experiment. It was observed that the influence zone of the contour in the PLAXIS model was much larger than the experiment. While the displacements observed in the PLAXIS models are higher, the trends observed in the experiments and the PLAXIS model are comparable. The shape of the influence zone changed from a triangular wedge to a circular arc failure as was seen in the experiments.

The differences in displacements in all three models when compared to their experiments can be due to the assumptions of a constant average stiffness in the Mohr-Coulomb model. Since the model does not take the higher unloading stiffness into account, higher lateral displacements and lower settlements are observed in the PLAXIS model. The larger influence zone observed in the model is because the Mohr-Coulomb model does not take strain-dependent stiffness into account. While stiffness at points away from the sheetpile are higher due to lower strain levels at these points, the Mohr-Coulomb model assumes a constant stiffness in the entire model. Hence, the displacements are larger in areas away from the sheetpile, leading to an influence zone that is larger than what is observed in the experiment. The differences in displacement trends and the size of the influence zone explained above were observed by researchers who evaluated the constitutive soil models for predicting lateral soil movements caused by deep excavations in sands (Hsiung and Dao, 2014; Sy-Dan, 2015). While the PLAXIS models over-predict the displacements and the failure zones in the models, the model still captures the displacement trend and failure shape obtained in the experiment and can hence be used as a first approximation of the behavior of the vegetation-sheetpile retaining system.

5

CONCLUSION

5.1. OVERVIEW

This thesis used 3D printed root analogues made of Poly-lactic Acid (PLA) in the place of real roots in embankments, to understand the effect of vegetation on stabilizing embankments and its role in the load sharing mechanism between the embankment, sheetpile and plant roots and also to analyse the ability of artificial roots to replace real roots in experiments to improve repeat-ability of tests. The mechanical properties of the material used in this experiment are comparable to mechanical properties the natural roots. The root architecture used in this model was a simplified model of the root architecture of the *Humulus lupulus* L. plant.

Three tests were performed to compare the performance of a bare embankment and rooted embankment. Two rooted patterns were used, where the distance from the sheetpile was varied and the number of roots within the failure plane were increased. The bare soil embankment failed at a draw-down depth of 120mm. The width of the failure wedge was found to be 100 mm extending to a depth of 200 mm. Based on the failure wedge obtained in the bare soil, two artificially printed roots were placed at a distance of 180 mm from the sheetpile with the horizontal root elements extending 100 mm on each side while a third root was placed at a distance of 380 mm from the sheetpile. The two roots in the first row were placed at a distance of 180 mm from each other. In the second model, the roots were placed at a distance of 1 cm from the sheetpile and the number of roots were increased from 3 to 5, with 3 roots in the first row with a spacing of 25 mm between them and 2 roots were placed in the second row, which was positioned at a distance of 8cm from the sheetpile. The rooted area hence extended along the entire width of the embankment.

WHAT IS THE EFFECT OF INCLUSION OF VEGETATION IN A SHEETPILE RETAINING SYSTEM

The observations from the experiment and the analytical models suggest that the stability of the embankment is improved in the presence of root elements. The root elements buttress the movement of the surrounding soil. The extent of vegetation within

the influence zone bench marked in the bare embankment determined the stability of the sheetpile vegetation system.

WHAT IS THE INFLUENCE OF ROOT AREA ON THE INCREASE IN STABILITY OF STREAM BANKS

While the presence of the root elements improved the performance of the embankment under draw-down conditions in the case of root pattern 1, it was seen that the minimal root area within the influence zone was not enough to stabilize the embankment. The embankment failed, though it was stable for a higher draw-down depth as compared to the bare soil embankment. The failure engaged a larger volume of soil and was an intact sliding block, compared to the block failure in the bare embankment.
When the rooted area in the influence zone of the embankment was increased, the performance of the embankment improved significantly. The displacements of the embankment were significantly reduced and remained stable for the entire draw-down depth of 250 mm.
It could hence be suggested that the presence of an increased root area along the entire width of the embankment, improved the stability of the embankment and the performance of the sheetpile-vegetation system.

5

ARE ARTIFICIAL ROOTS AN ALTERNATIVE TO REAL VEGETATION FOR FUTURE STUDIES

The root models used in the experiments were printed using the Poly Lactic Acid, whose mechanical properties were comparable to the root of the *Humulus lupulus* L. plant. Each root model could be printed in 6 hours to be used for testing. This certainly helps to improve the repetition of the experiments. The results from the experiments at 1g with the root analogues were comparable to the results of tests conducted using live vegetation in a centrifuge at higher g (Mickovski et al, 2009; Sonnenberg et al, 2010;2012; Liang, 2015).
The physical models were validated using a finite element model developed using PLAXIS. The Mohr-Coulomb model was used to model the behaviour of the soil system. The vegetated area in the embankment was represented as a cuboidal area with an increased cohesion. While the displacements and the failure wedge observed in the PLAXIS model were comparatively higher than the displacements observed in the experiments, the models were able to predict the behaviour of the three systems and the capture the failure accurately. The higher displacements can be attributed to the constitutive model used predict the behaviour of the system, which assumes a uniform stiffness for the soil across the entire model.

DOES EQUIVALENT COHESION APPROACH TO ROOT MODELLING CAPTURE THE EFFECT OF VEGETATION

On comparing the results of the bare soil model and the rooted models, the effect of vegetation provided as an increase in cohesion improved the stability of the embankment. The root area was modelled with the equivalent cohesion approach where the rooted area was modelled as a cuboidal area. The cuboidal shape of the rooted area involves the use of a lesser number of elements as compared to the other geometrical approximations developed for root structures (Kostler et al, 1968). This helps reduce the complexities and also the computation time of the model. Das (2015) modelled vegetation

using the equivalent cohesion approach, in his study of slope stability analysis with vegetation in PLAXIS 3D. It was observed that slopes with vegetation showed an increased FS as compared to bare slopes. By placing the rooted area within the area of influence observed from the bare soil model, the stability of the system was improved.

5.2. RECOMMENDATIONS FOR FUTURE WORK

1. The support structure for the root elements are printed using the same material as the root elements, which eventually have to be broken off. Hence, small elements which are printed risk being broken off when removing the support structure. ABS is a 3D printing material which uses a support structure can be dissolved in an acid bath. This technique allows a more elaborate design to be printed. This technique could be investigated for printing the root elements.

2. The Mohr-Coulomb model used to model the experiment is a good first approximation of the behaviour of the system. The Hardening soil model uses a wider range of input parameters and offers a more accurate representation of soil behaviour. The system could be modelled using the HS model for a more accurate representation of soil behaviour.

3. While this 1g experiment done with artificial roots yielded similar displacement trends and failure as the tests done on live plants and artificial roots in scaled down models in a centrifuge, it does not have other experiments in 1g with live plants which can be used as a comparison. Hence similar experiments could be performed with live plants at 1g, which would help to further validate the approach used in this study.

BIBLIOGRAPHY

[1] T Endo and T Tsuruta. "Effects of tree root upon the shearing strengths of soils". In: *Annual Report of the Hokkaido Branch, Tokyo Forest Experiment Station* 18 (1969), pp. 168–179.

[2] Donald H Gray. "Reinforcement and stabilization of soil by vegetation". In: *Journal of Geotechnical and Geoenvironmental Engineering* 100.Proc Paper 10597 Tech Notes (1974).

[3] Tien H Wu. *Investigation of landslides on prince of Wales Island, Alaska*. Ohio State University, 1976.

[4] LJ Waldron. "The shear resistance of root-permeated homogeneous and stratified soil". In: *Soil Science Society of America Journal* 41.5 (1977), pp. 843–849.

[5] Tien H Wu, William P McKinnell III, and Douglas N Swanston. "Strength of tree roots and landslides on Prince of Wales Island, Alaska". In: *Canadian Geotechnical Journal* 16.1 (1979), pp. 19–33.

[6] Nick J Coppin and Ivor G Richards. *Use of vegetation in civil engineering*. Ciria Butterworths, 1990.

[7] Ronald J Adrian. "Particle-imaging techniques for experimental fluid mechanics". In: *Annual review of fluid mechanics* 23.1 (1991), pp. 261–304.

[8] Weimin Wu and Roy C Sidle. "A distributed slope stability model for steep forested basins". In: *Water resources research* 31.8 (1995), pp. 2097–2110. DOI: 10.1029/95WR01136.

[9] D.H. Gray and R.B. Sotir. *Biotechnical Soil Bioengineering Slope Stabilization: A Practical Guide for Erosion Control*. John Wiley Sons, 1996. ISBN: 0471049786, 9780471049784.

[10] J-W.G. van de Kuilen M.L.R. van der Linden. "Reliability Based Design Of Timber Sheet Pile Walls". In: *NZ TIMBER DESIGN JOURNAL* (1999), pp. 134–143. DOI: 10.1016/j.compgeo.2007.04.001.

[11] DJ White et al. "A deformation measurement system for geotechnical testing based on digital imaging, close-range photogrammetry, and PIV image analysis". In: *Proceedings of the International Conference on Soil Mechanics and Geotechnical Engineering*. Vol. 1. AA Balkema Publishers. 2001, pp. 539–542.

[12] VNS Murthy. *Geotechnical engineering: principles and practices of soil mechanics and foundation engineering*. CRC press, 2002.

[13] Roy PC Morgan and R Jane Rickson. *Slope stabilization and erosion control: a bioengineering approach*. Taylor & Francis, 2003.

[14] Kanji Kondo et al. “Analytical study on the role of tree roots system in slope stability”. In: *Journal of the Japan Landslide Society* 41.3 (2004), pp. 255–263.

[15] N. Pollen and A. Simon. “Estimating the mechanical effects of riparian vegetation on stream bank stability using a fiber bundle model.” In: *Water Resour. Res.* 41 (2005). DOI: 10.1029/2004WR003801.

[16] K. V. Babu B. V. S. Viswanadham S. P. G. Madabhushi and V. S. Chandrasekaran. “Modelling the failure of a cantilever sheetpile wall”. In: *International Journal of Geotechnical Engineering* (2007), pp. 215–231. DOI: DOI10.3328/IJGE.2009.03.02.215-231.

[17] B.M. Basha G.L.S. Babu. “Optimum design of cantilever sheet pile walls in sandy soils using inverse reliability approach”. In: *Computers and Geotechnics* (2008), pp. 134–143. DOI: 10.1016/j.compgeo.2007.04.001.

[18] Marie Genet et al. “Root reinforcement in plantations of Cryptomeria japonica D. Don: effect of tree age and stand structure on slope stability”. In: *Forest ecology and Management* 256.8 (2008), pp. 1517–1526.

[19] Slobodan B Mickovski et al. “Mechanical reinforcement of soil by willow roots: impacts of root properties and root failure mechanism”. In: *Soil Science Society of America Journal* 73.4 (2009), pp. 1276–1285.

[20] Natasha Pollen-Bankhead and Andrew Simon. “Hydrologic and hydraulic effects of riparian root networks on streambank stability: Is mechanical root-reinforcement the whole story?” In: *Geomorphology* 116.3-4 (2010), pp. 353–362. DOI: 10.1016/j.geomorph.2009.11.013.

[21] M Schwarz, D Cohen, and Dani Or. “Root-soil mechanical interactions during pullout and failure of root bundles”. In: *Journal of Geophysical Research: Earth Surface* 115.F4 (2010). DOI: 10.1029/2009JF001603.

[22] R Sonnenberg et al. “Centrifuge modelling of soil slopes reinforced with vegetation”. In: *Canadian Geotechnical Journal* 47.12 (2010), pp. 1415–1430. DOI: 10.1139/T10-037.

[23] Faisal Hj. Ali Khalilnejad A. and N. Osman. “Contribution of the Root to Slope Stability.” In: *Geotech Geol Eng* (2012), pp. 277–288. DOI: https://doi.org/10.1007/s10706-011-9446-5.

[24] R Sonnenberg et al. “Centrifuge modelling of soil slopes containing model plant roots”. In: *Canadian Geotechnical Journal* 49.1 (2012), pp. 1–17.

[25] Chris RI Clayton et al. *Earth pressure and earth-retaining structures*. CRC press, 2014.

[26] Kreng Hav Eab, A Takahashi, and S Likitlersuang. “Centrifuge modelling of root-reinforced soil slope subjected to rainfall infiltration”. In: *Géotechnique Letters* 4.3 (2014), pp. 211–216.

[27] Chia-Cheng Fan and Yi-Fan Lai. “Influence of the spatial layout of vegetation on the stability of slopes”. In: *Plant and soil* 377.1-2 (2014), pp. 83–95. DOI: 10.1007/s11104-012-1569-9.

[28] Tobias GRAF et al. “Humulus lupulus–The hidden half”. In: *BrewingScience* 67.11/12 (2014), pp. 161–166.

[29] BC Hsiung and Sy-Dan Dao. “Evaluation of constitutive soil models for predicting movements caused by a deep excavation in sands”. In: *Electronic J. Geotech. Eng* 1 (2014), pp. 17325–17344.

[30] A Askarinejad and Sarah M Springman. “Centrifuge modelling of the effects of vegetation on the response of a silty sand slope subjected to rainfall”. In: *Computer Methods and Recent Advances in Geomechanics: Proceedings of the 14th International Conference of International Association for Computer Methods and Recent Advances in Geomechanics, 2014 (IACMAG 2014)*. Taylor & Francis Books Ltd. 2015, pp. 1339–1344.

[31] S. Das. “Quantifying the role of vegetation in slope stability”. In: 2015.

[32] Bin-Chen Benson Hsiung and Sy-Dan Dao. “Prediction of Ground Surface Settlements Caused by Deep Excavations in Sands”. In: *Geotechnical Engineering* 46.3 (2015), pp. 111–118.

[33] T. Liang. “Seismic performance of vegetated slopes”. University of Dundee, 2015, pp. 1–209.

[34] Ng C.W.W. Liu H.W. Feng S. “Analytical analysis of hydraulic effect of vegetation on shallow slope stability with different root architectures”. In: *Computers and Geotechnics* (2016), pp. 115–120. DOI: 10.1016/j.compgeo.2016.06.006.

[35] Charles Wang Wai Ng et al. “A new and simple water retention model for root-permeated soils”. In: *Géotechnique Letters* 6.1 (2016), pp. 106–111. DOI: 10.1680/jgele.15.00187.

[36] Yuanjun Yang et al. “Effect of root moisture content and diameter on root tensile properties”. In: *PLoS One* 11.3 (2016), e0151791.

[37] Teng Liang et al. “Scaling of the reinforcement of soil slopes by living plants in a geotechnical centrifuge”. In: *Ecological Engineering* 109 (2017), pp. 207–227.

[38] JJ Ni et al. “Modelling hydro-mechanical reinforcements of plants to slope stability”. In: *Computers and Geotechnics* 95 (2018), pp. 99–109. DOI: 10.1016/j.compgeo.2017.09.001.